

The Largest Inscribed Triangle and
the Smallest Circumscribed Triangle of a Convex Polygon:
An Overview of Linear-Time Algorithms

Günter Rote

Extended Class Notes, June 3, 2019

Contents

B1			
B2			
B3			
B4			
B5			
B6			
B7	1	Setup for the largest inscribed triangle	2
B8	2	Finding the largest anchored triangle	2
B9	2.1	The largest anchored triangle is unique	3
B10	2.2	The local problem with a triangular outer polygon	3
B11	2.3	The direction of improvement for the largest anchored triangle	5
B12	3	The smallest anchored circumscribed triangle	7
B13	4	How B^* and C^* move when the direction is rotated	8
B14	5	How the area changes when the direction is rotated	11
B15	6	How the motion continues after a breakpoint	11
B16	7	A linear-time algorithm for the Circular Sweep	13
B17	8	Speed-up for the largest inscribed triangle	14
B18	8.1	The Skipping Algorithm	14
B19	8.2	Simplifying the test: Jin's Algorithm	15
B20	8.3	Correctness, termination, and running time	16
B21	9	Speed-up for the smallest circumscribed triangle	17
B22	A	Literature	22
B23	B	Primitive operations	23
B24	B.1	The area of the parallelogram spanned by two vectors	23
B25	B.2	The improvement test for anchored triangles	24
B26	B.2.1	Algebraic calculation of the sign of the derivative of $f(h)$	24
B27	B.2.2	Geometric constructions of the improvement test	25
B28	B.3	Finding the next breakpoint	25
B29	B.3.1	Algebraic computation of the next breakpoint	25
B30	B.3.2	Computation and construction of the next breakpoint in the literature	26
B31	B.4	The degree of the predicates	26
B32	B.5	The area of the circumscribed triangle	26
B33	C	Constructing the largest anchored inscribed triangle from the smallest an-	
B34		chored circumscribed triangle	27
B35	D	An alternative proof that B^* and C^* move monotonically	28

B36

1 Setup for the largest inscribed triangle

B37

We are given a convex polygon P with n vertices in counterclockwise order. We look for a triangle ABC of largest area contained in P . It is obvious that the corners A, B, C must lie on the boundary of P , and hence we speak of an *inscribed* triangle.

B38

B39

B40

B41

B42

B43

B44

B45

Our approach is to solve a constrained problem where the direction of the edge BC is specified. More precisely, for a given direction vector $\mathbf{u} = \mathbf{u}(\theta) = \begin{pmatrix} \cos \theta \\ \sin \theta \end{pmatrix}$, we look for the largest inscribed triangle among the triangles ABC for which \mathbf{u} is the outer normal of the edge BC , see Figure 2a for an illustration. We call such triangles ABC *anchored at \mathbf{u}* , and we denote the *largest* such triangle by $A^*B^*C^* = A^*(\theta)B^*(\theta)C^*(\theta)$. We always label ABC in counterclockwise order.

B46

B47

B48

B49

The idea is now to sweep the direction θ through the full range of possible angles and maintain the triangle $A^*(\theta)B^*(\theta)C^*(\theta)$ along the way. The largest inscribed triangle must be encountered during this *Circular Sweep*. A nice animation of this process can be seen in [Kal, Figure 1].

B50

B51

B52

B53

It is clear that the corner A^* is the extreme vertex in direction $-\mathbf{u}$.¹ As we rotate the direction θ counterclockwise, the point $A^*(\theta)$ will jump from one vertex to the next in counterclockwise direction whenever $-\mathbf{u}(\theta)$ is the outer normal of a polygon edge. For the other two points, we have the following crucial properties.

B54

1. The points $B^*(\theta)$ and $C^*(\theta)$ are unique (Lemma 1).

B55

B56

2. The points $B^*(\theta)$ and $C^*(\theta)$ move monotonically in counterclockwise direction on the boundary of the polygon as θ is increased. (Theorem 5.ii.)

B57

B58

B59

B60

B61

We will see how to maintain $B^*(\theta)$ and $C^*(\theta)$ as θ ranges over the interval $[0^\circ \dots 360^\circ]$. We have to process a linear number of events, and for each event, we can carry out the elementary steps and decisions of the process in constant time. Figure 1 shows an example how the area of $A^*(\theta)B^*(\theta)C^*(\theta)$ varies depending on θ .² By picking the maximum of this function, we find the largest inscribed triangle in linear time.

B62

2 Finding the largest anchored triangle

B63

B64

B65

B66

B67

B68

B69

B70

We consider a fixed direction \mathbf{u} . We parameterize the triangle $A^*BC = A^*B(h)C(h)$ by the height h over the side BC , see Figure 2a. For a given height h , the segment $B(h)C(h)$ is determined as the intersection of the area of P with the line perpendicular to \mathbf{u} at distance h from A^* . The variable h ranges between 0 and the width $w(\mathbf{u})$ of the polygon in direction \mathbf{u} . In particular, if P has an edge with outer normal \mathbf{u} , then $B(h)C(h)$ for $h = w(\mathbf{u})$ is equal to that edge, see Figure 5b. Since this case sometimes requires special arguments, we give it a name: We call an edge of P the *\mathbf{u} -extreme edge* if its outer normal is \mathbf{u} . (For most directions \mathbf{u} , there is no \mathbf{u} -extreme edge.)

B71

B72

B73

B74

It may happen that A^* is not unique, namely when the polygon has an edge with outer normal $-\mathbf{u}$, see Figure 2b. In this case, it does not matter which point A^* we pick from that edge: This choice affects neither the definition of $B(h)$ and $C(h)$ nor the area of the triangle $A^*B(h)C(h)$.

B75

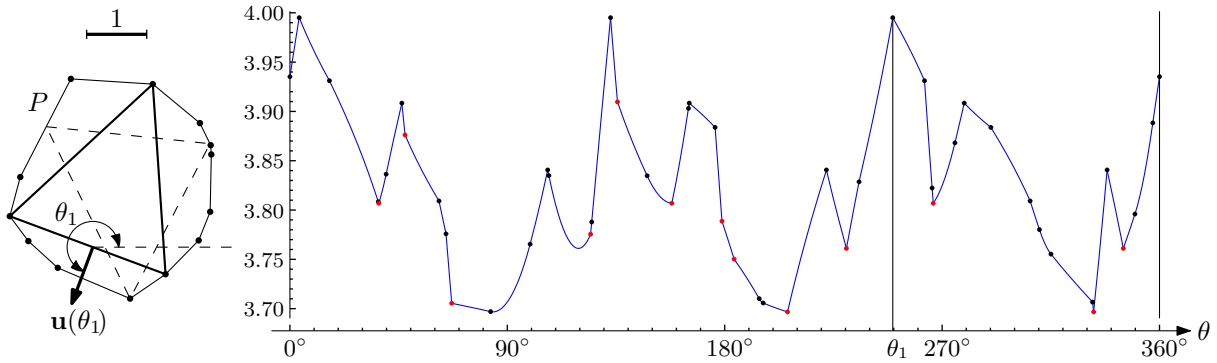
B76

B77

B78

¹In Kallus [Kal], anchored triangles with this corner A^* are called “candidate-anchored triangles”. His “anchored triangles” are what we call *largest anchored triangles*.

²This polygon is instance number 18 in the test suite that Kallus [Kal] provided with the source files of his arXiv preprint and at <https://github.com/ykallus/max-triangle/releases/tag/v1.0>



B79 Figure 1: The area $F(\theta)$ of the largest θ -anchored triangle $A^*(\theta)B^*(\theta)C^*(\theta)$ as a function of
 B80 the direction $\theta \in [0^\circ \dots 360^\circ]$, for the 13-gon P shown on the left. This function is piecewise
 B81 smooth and continuous. The 47 dots on the graph, excluding the boundaries at 0° and 360° ,
 B82 are the breakpoints where the combinatorial type changes in the sense that a triangle corner
 B83 moves to a different polygon edge or rests at a polygon vertex. (One black dot is almost hidden
 B84 behind the first red dot.) The 13 red breakpoints correspond to the inner normals of the edges,
 B85 where A^* jumps from one vertex to the next. The largest inscribed triangle in P is shown. It
 B86 is encountered three times as a maximum of $F(\theta)$, namely whenever $\mathbf{u}(\theta)$ is one of the outer
 B87 normals of this triangle. The direction θ_1 where this happens for the third time is indicated.
 B88 The dashed triangle in P corresponds to the three minima of $F(\theta)$. We will see in Section 3
 B89 that it determines the smallest circumscribed triangle of P .

B90 2.1 The largest anchored triangle is unique

B91 **Lemma 1.** *The function $f: [0 \dots w(\mathbf{u})] \rightarrow \mathbb{R}_{\geq 0}$ defined by $f(h) = \text{area } A^*B(h)C(h)$ is continuous
 B92 and unimodal: It starts from $f(0) = 0$ with a strictly increasing part; it has a unique maximum;
 B93 and this is followed by a strictly decreasing part. The decreasing part may be missing.*

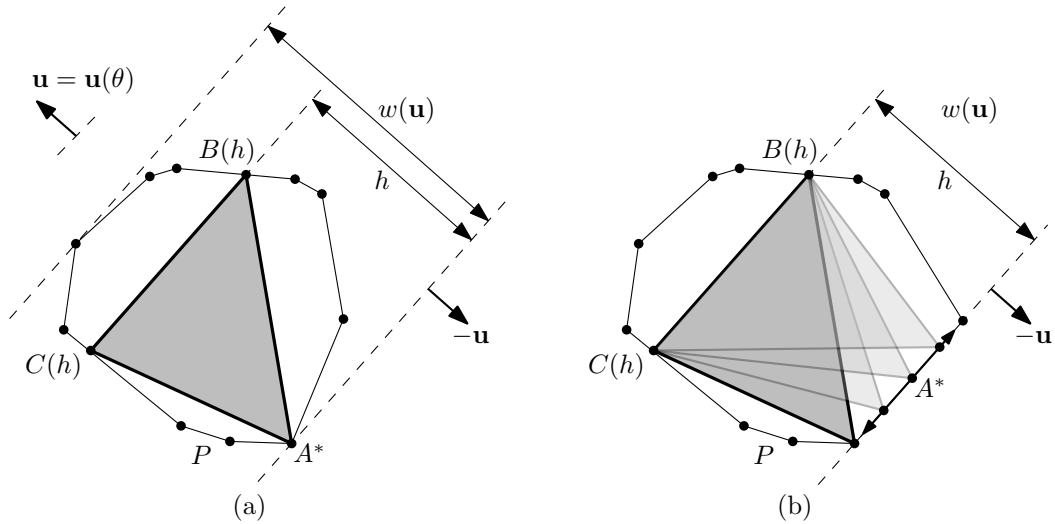
B94 *Proof.*³ The area $f(h) = \frac{1}{2}h|B(h)C(h)|$ is $\frac{1}{2}$ times the product of the height h and the baseline
 B95 $|B(h)C(h)|$ of the triangle. Since both factors are continuous between 0 and $w(\mathbf{u})$, f is continuous
 B96 as well. Due to the convexity of P , the length $g(h) := |B(h)C(h)|$ is a concave function, and
 B97 it consists of a weakly increasing part between $h = 0$ and some h_{\max} where it achieves the
 B98 maximum, and a decreasing part between h_{\max} and $w(\mathbf{u})$. In the first part, $f(h) = \frac{1}{2}h \cdot g(h)$ is
 B99 the product of h with a weakly increasing positive function, and is therefore strictly increasing.
 B100 In the second part, we look at the derivative $f'(h) = \frac{1}{2}(g(h) + h \cdot g'(h))$. The function g is not
 B101 differentiable everywhere, but we can take the right derivative in this equation. The function g
 B102 is strictly decreasing, and the second term is the product of h with a negative piecewise constant
 B103 decreasing function. Both terms are strictly decreasing. So the function f' is strictly decreasing,
 B104 and the function f is strictly concave and therefore unimodal in the second part.

B105 Since $f(0) = 0$, the increasing part is always present. The decreasing part may be missing
 B106 when the polygon P has an edge with outer normal \mathbf{u} . □

B107 2.2 The local problem with a triangular outer polygon

B108 The range of the function f is decomposed into pieces. On each piece, $B(h)$ and $C(h)$ slide
 B109 along two fixed edges b and c of P . In order to analyze the behavior of f on one of these pieces,
 B110 we first consider the case that $B(h)$ and $C(h)$ range over two lines b and c .

B111 ³See [Kal, Lemma 2.2-3] for a different, less elementary proof of the unique maximum property. (The term
 B112 “convex” should be read as “concave” or “downward convex”.)

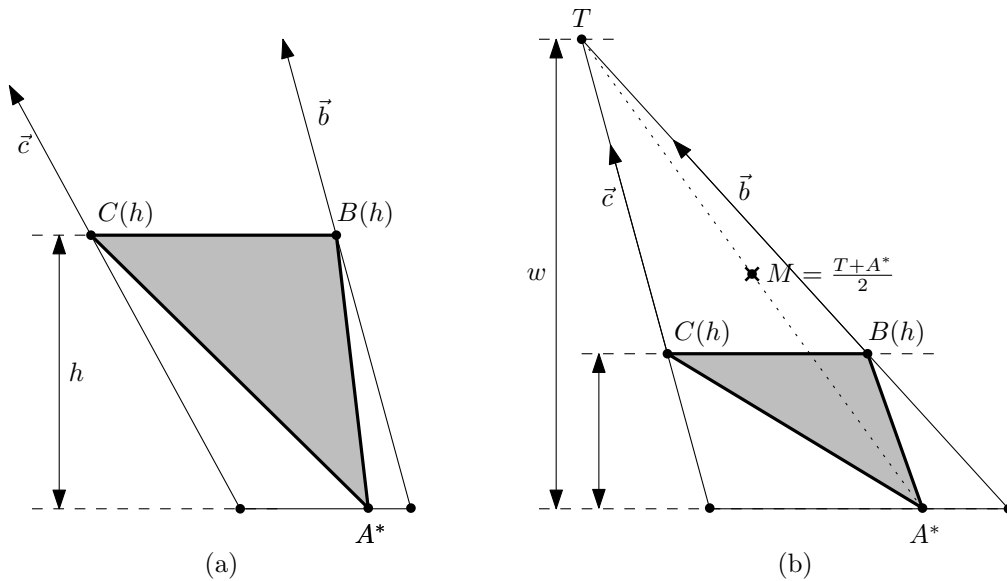


B113 Figure 2: (a) Notations for anchored triangles $A^*B(h)C(h)$. (b) Moving A^* parallel to BC does not affect the area of A^*BC .

B114 To facilitate the discussion, we assume in this section and whenever it is convenient that $\theta =$
 B115 90° and \mathbf{u} points in the upward direction. This allows us to use the words “above” and “below”,
 B116 “up” and “down” with reference to this situation. They have to be interpreted appropriately when
 B117 \mathbf{u} is rotated.

B118 Thus, we are looking for a triangle A^*BC with a horizontal edge BC that lies above A^* ,
 B119 where B and C are constrained to lie on two upward rays \vec{b} and \vec{c} and C should be to the left
 B120 of B , see Figure 3.

B121 **Lemma 2.** *The area of A^*BC is a quadratic function of h . If the rays \vec{b} and \vec{c} don't meet, then*
 B122 *the area increases indefinitely with h , and there is no largest triangle. Otherwise, the area of*
 B123 *A^*BC has a unique maximum, which is found as follows: let T be the intersection of \vec{b} and \vec{c} .*
 B124 *Then the edge B^*C^* of the largest triangle goes through the midpoint M of T and A^* .*



B125 Figure 3: The largest anchored triangle restricted by two rays \vec{b} and \vec{c}

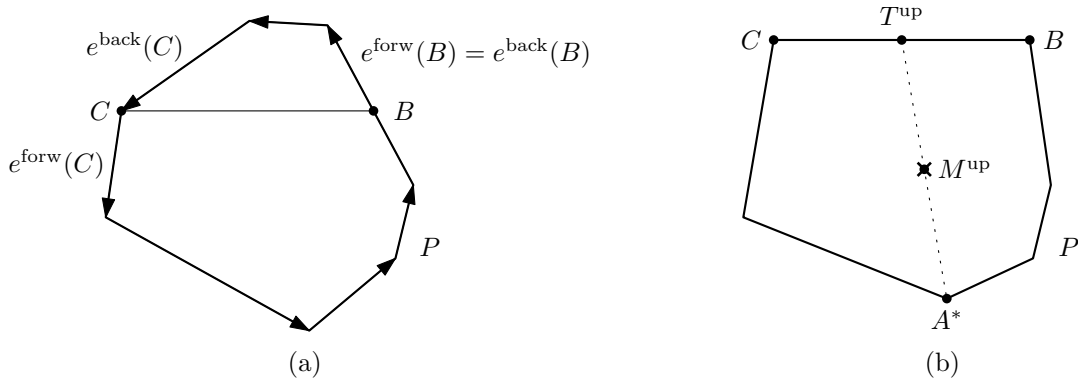
B126 *Proof.* The area $f(h) = \frac{1}{2}h|B(h)C(h)|$ is $\frac{1}{2}$ times the product of the height h and the baseline
 B127 $|B(h)C(h)|$ of the triangle. If the rays \vec{b} and \vec{c} are parallel or diverge, then it is clear that the area
 B128 increases without bounds, since h increases and the baseline $|B(h)C(h)|$ increases or remains
 B129 constant, see Figure 3a.

B130 Otherwise, the length of the baseline $B(h)C(h)$ is proportional to $w - h$, where w is the
 B131 vertical distance between T and A^* , see Figure 3b. It follows that $f(h) = \frac{1}{2}h|B(h)C(h)|$ has
 B132 the form $f(h) = \alpha h(w - h)$ for some constant α , and this is maximized for $h = w/2$. This is
 B133 precisely the value h where the segment $B(h)C(h)$ goes through the midpoint $(T + A^*)/2$. \square

B134 **Definition.** We call $M = (T + A^*)/2$ the *critical pivot point* or simply the *critical point*.

B135 The usefulness of the above lemma results from the way in which the optimality criterion
 B136 is phrased: When \mathbf{u} is rotated, the critical point remains fixed as long as A^* remains fixed,
 B137 whereas w and h change.

B138 2.3 The direction of improvement for the largest anchored triangle

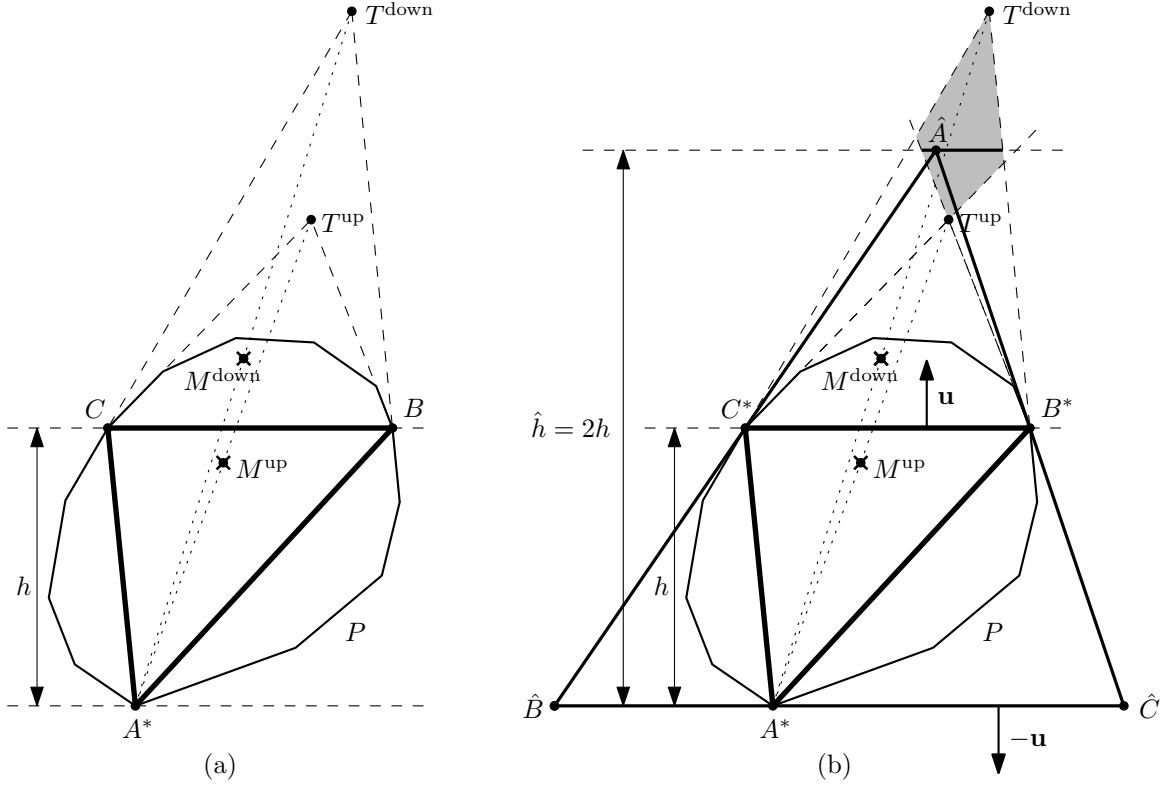


B139 Figure 4: (a) The forward and backward incident edges of a point on the boundary of P .
 B140 (b) A possible definition of M^{up} when BC is an edge of P

B141 We now return to the situation when B and C are restricted to the original polygon P . To
 B142 check whether the triangle ABC is largest, we use Lemma 2. If B or C is at a vertex of P , the
 B143 function $f(h)$ is not differentiable at this point, and we have to look at its one-sided derivatives.
 B144 For a point B (or C) that is a vertex of P , we call its two incident edges the *forward edge*
 B145 $e^{\text{forw}}(B)$ and the *backward edge* $e^{\text{back}}(B)$, according to the counterclockwise orientation of P ,
 B146 see Figure 4a. If B lies in the interior of an edge e of P , we define $e^{\text{forw}}(B)$ and $e^{\text{back}}(B)$ to be
 B147 that same edge e .

B148 If we consider the behavior of $f(h)$ when h is increased, we have to look at the upward
 B149 rays through the two *upper* incident edges $e^{\text{forw}}(B)$ and $e^{\text{back}}(C)$. We denote their intersection
 B150 by T^{up} , if it exists, and the midpoint between this point and A^* is the *upward critical pivot*
 B151 *point* M^{up} , see Figure 5a. Accordingly we define the *downward critical pivot point* M^{down} by
 B152 the upward rays through the two *lower* incident edges $e^{\text{back}}(B)$ and $e^{\text{forw}}(C)$. If neither B nor
 B153 C is a vertex of P , then M^{up} and M^{down} coincide. Otherwise, M^{up} lies *below* M^{down} , despite
 B154 what the name suggests!

B155 More generally, we will repeatedly compare critical points that are defined by pairs of edges.
 B156 It will be good to remember that exchanging one of the defining edges by another edge further
 B157 *down* causes the defining ray to bend *outward*. Hence the critical point will move *upward*, or
 B158 cease to exist.



B159 Figure 5: (a) The optimality criterion for a largest anchored triangle A^*BC . (b) An anchored
 B160 circumscribed triangle $\hat{A}\hat{B}\hat{C}$ corresponding to a largest anchored inscribed triangle A^*BC . More
 B161 typically, the gray feasible arcs for \hat{A} degenerates to a line segment or ray or to a single point.

B162 By Lemma 2, the critical point M , if it exists, gives the direction in which BC has to move
 B163 in order to increase the area, according to the following *Improvement Test*:

B164 We should increase h if and only if M^{up} lies above BC . (1)

B165 We should decrease h if and only if M^{down} lies below BC . (2)

B166 As a memory aid, one can remember that BC wants to move *close* to the critical point.

B167 The intersection T , and hence the critical point M , may not exist, and in that case, h should
 B168 be increased if we want to increase the area. We can remember that, if the rays don't intersect,
 B169 and hence the critical point does not exist, it is always consistent with (1) to treat this case *as*
 B170 *if the critical point would lie above BC* . Nevertheless, we will always explicitly mention the case
 B171 of nonexistence in the statements of the lemmas, at least parenthetically.

B172 **Lemma 3** (Optimality criterion for an anchored triangle). *The inscribed triangle A^*BC with*
 B173 *height h and side BC perpendicular to \mathbf{u} is the optimum anchored triangle if and only if $h > 0$*
 B174 *and the following two conditions are satisfied:*

B175 a) *The downward critical point M^{down} lies on or above BC (or does not exist).*

B176 b) *If h does not lie at the maximum of its range,*
 B177 *the upward critical point M^{up} lies on or below BC .*

B178 *Proof.* The conditions are the necessary conditions for a local maximum of $f(h)$: Condition (a)
 B179 looks at the left derivative, and Condition (b) looks at the right derivative. The case when h
 B180 is at the maximum of its range is treated specially in Condition (b) because there is no right

B181 derivative. When the critical point lies *on* the segment BC , the derivative is 0. Nevertheless,
 B182 this is sufficient to conclude that the area cannot be increased by moving h in that direction,
 B183 since the quadratic function $f(h)$ has then a critical point at h , and this critical point is a
 B184 maximum.

B185 For $h \rightarrow 0$, the area decreases to 0, and hence the optimum must occur at a positive height.
 B186 By Lemma 1, the maximum is unique, and therefore the conditions are also sufficient. \square

B187 We mention that an alternative proof of Lemma 1 (uniqueness of B^* and C^*) can be obtained
 B188 by arguing directly that the necessary conditions (a) and (b) can have at most one solution.⁴

B189 3 The smallest anchored circumscribed triangle

B190 We relate the largest inscribed triangle anchored at \mathbf{u} to the *smallest-area circumscribed triangle*
 B191 $\hat{A}\hat{B}\hat{C}$ among the triangles *anchored at* $-\mathbf{u}$, in the sense that $-\mathbf{u}$ is the outer normal of the
 B192 edge $\hat{B}\hat{C}$.⁵

B193 **Lemma 4.** *i) Let $A^*B^*C^*$ be a largest inscribed triangle anchored at \mathbf{u} , of height h . Then*
 B194 *the smallest circumscribed triangle $\hat{A}\hat{B}\hat{C}$ anchored at $-\mathbf{u}$ has height $\hat{h} = 2h$, and the length*
 B195 *of its baseline is $\hat{B}\hat{C} = 2 \cdot B^*C^*$, and hence its area is 4 times the area of $A^*B^*C^*$.*

B196 *ii) There is always a smallest anchored circumscribed triangle $\hat{A}\hat{B}\hat{C}$ such that the side $\hat{A}\hat{B}$ or*
 B197 *the side $\hat{A}\hat{C}$ touches a whole edge of P .⁶*

B198 *Proof.* Figure 5b shows how $\hat{A}\hat{B}\hat{C}$ is constructed. Again we assume without loss of generality
 B199 that \mathbf{u} points vertically upward. From an appropriate point \hat{A} at height $2h$ above A^* , we put
 B200 tangents to P through the points B^* and C^* and we extend these tangents until they meet the
 B201 horizontal line through A^* in the points \hat{C} and \hat{B} , respectively. Then $\hat{B}\hat{C} = 2 \cdot B^*C^*$, because
 B202 the triangles $\hat{A}\hat{B}\hat{C}$ and $\hat{A}C^*B^*$ are similar and the ratio of their heights is 2.

B203 We must show that a point \hat{A} with the desired properties exists. The requirement that the
 B204 tangents from \hat{A} should touch P in the points B^* and C^* restricts \hat{A} to the intersection of two
 B205 wedges (the shaded area in Figure 5b). Its boundary is formed by at most four edges. By
 B206 definition, the lowest point of the region is T^{up} , and from Condition (b) of Lemma 3, this point
 B207 exists and lies below the line at height $2h$. The highest point is T^{down} , if that point exists, or
 B208 otherwise the region is unbounded. Thus, by Condition (a) of Lemma 3, the region extends
 B209 above the line at height $2h$. Thus, a point \hat{A} at height $2h$ in this region can be found. In
 B210 Figure 5b, The possible choices for \hat{A} are highlighted.

B211 Choosing \hat{A} at the boundary of the allowed region ensures that one side of the triangle
 B212 touches a whole edge of P , thus proving the second statement of the lemma.

B213 We still need to show that there is no smaller anchored triangle containing P . In fact, there
 B214 is not even a smaller anchored triangle that contains just the triangle $A^*B^*C^*$: This statement
 B215 is dual to Lemma 2, and its proof is just as easy, see Figure 6. If we choose the point \hat{A} at some
 B216 height \hat{h} , the smallest anchored circumscribed triangle must contain the projection of $\hat{B}\hat{C}$ of the
 B217 segment C^*B^* from \hat{A} to the horizontal line through A^* , and by similar triangles, the base $\hat{B}\hat{C}$

B218 ⁴Consider the points M^{up} and M^{down} as h increases from 0 to the maximum value. After an initial period
 B219 where the points don't exist and therefore M^{up} and M^{down} "lie above" BC , the critical points move downwards
 B220 because the edges incident to B and C turn more and more inwards. At the same time the edge BC moves
 B221 upwards. Thus, there can be only one point where (a) and (b) are fulfilled and the interval between M^{up} and
 B222 M^{down} straddles the segment BC . The precise argument is a bit delicate because of the jumps of M^{up} and M^{down} .

B223 ⁵The strong connection between the two problems was first explicitly noted and exploited by Chandran and
 B224 Mount, see in particular [ChMo, Lemma 2.4 in connection with Lemma 2.5]. The statement of our Lemma 4.i is
 B225 discussed after the proof of Lemma 2.4.

B226 ⁶[KLLa, Theorem 2.1.iv].

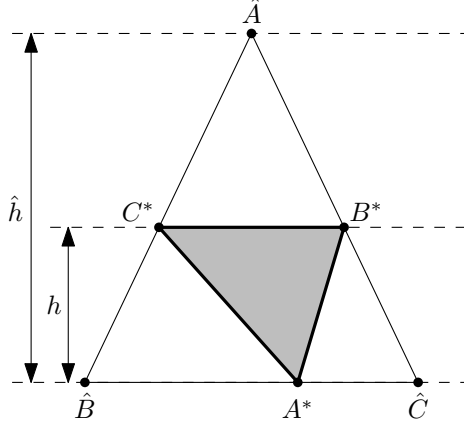


Figure 6: An anchored triangle containing $A^*B^*C^*$

B227

B228 is $\hat{h}/(\hat{h} - h)$ times as long as the segment C^*B^* , and hence the area of $\hat{A}\hat{B}\hat{C}$ is $\frac{1}{2} \cdot \hat{h} \cdot \frac{\hat{h}}{\hat{h}-h} B^*C^*$.
 B229 The minimum of this expression is achieved for $\hat{h} = 2h$. \square

B230 This lemma has a converse⁷: From a smallest circumscribed triangle $\hat{A}\hat{B}\hat{C}$ anchored at $-\mathbf{u}$,
 B231 one can recover a largest inscribed triangle $A^*B^*C^*$ anchored at \mathbf{u} . We don't need this direction,
 B232 but for completeness, it is proved in Appendix C (Lemma 14).

B233 The lemma shows that, by computing the area $A^*(\theta)B^*(\theta)C^*(\theta)$ for all directions θ , we can
 B234 simultaneously find the smallest circumscribed triangle: Instead of looking for the largest area
 B235 among these triangles, we just look for the smallest area, and we multiply the result by 4. (It
 B236 is a bit paradoxical that we should look for *largest* inscribed anchored triangles in order to find
 B237 the circumscribed triangle with *smallest* area.)

B238 4 How B^* and C^* move when the direction is rotated

B239 We define the *combinatorial type* of an inscribed triangle ABC as the specification that tells for
 B240 each of the three corners A, B, C on which vertex of P or in the interior of which edge of P it
 B241 lies.

B242 **Theorem 5.** *i) The domain of angles θ is partitioned into intervals at breakpoints $0^\circ = \theta_0 <$
 B243 $\theta_1 < \dots < \theta_i < \theta_{i+1} < \dots < \theta_k = 360^\circ$, such that in each open interval $(\theta_i \dots \theta_{i+1})$,
 B244 all triangles $A^*(\theta)B^*(\theta)C^*(\theta)$ have the same combinatorial type. Moreover, in each closed
 B245 interval $[\theta_i \dots \theta_{i+1}]$, the edge $B^*(\theta)C^*(\theta)$ pivots around a point M on this edge.⁸ There are
 B246 three mutually exclusive possibilities, which are illustrated in Figure 7.*

- B247 I. $M = B^*(\theta)$ is stationary at a vertex of P and $C^*(\theta)$ slides on a fixed edge of P .
- B248 II. $M = C^*(\theta)$ is stationary at a vertex of P and $B^*(\theta)$ slides on a fixed edge of P .
- B249 III. The critical pivot points M^{up} and M^{down} coincide, and $M^{\text{up}} = M^{\text{down}} =: M$ lies on
 B250 the segment B^*C^* ; the segment $B^*(\theta)C^*(\theta)$ rotates around M , and $B^*(\theta)$ and $C^*(\theta)$
 B251 slide on two fixed edges of P .⁹

B252 ⁷cf. [ChMo, Lemma 2.4]

B253 ⁸In the animation shown in [Kal, Figure 1], it is apparent that the optimal edges B^*C^* go through a common
 B254 point when \mathbf{u} is rotated in some range.

B255 ⁹See [ChMo, Figure 5], covering the case where the smallest anchored circumscribed triangle has “two flush
 B256 legs”. The pivot is the point x in that figure, and it is constructed by considering the local optimality condition
 B257 of the circumscribed triangle.

- B258 ii) Moreover, $B^*(\theta)$ and $C^*(\theta)$ move continuously and monotonically¹⁰ in counterclockwise
 B259 direction on the boundary of the polygon P as θ is increased. They make a full turn around
 B260 P as θ ranges over the interval $[0^\circ \dots 360^\circ]$.
- B261 iii) The number k of intervals is at most $5n + 1$.¹¹

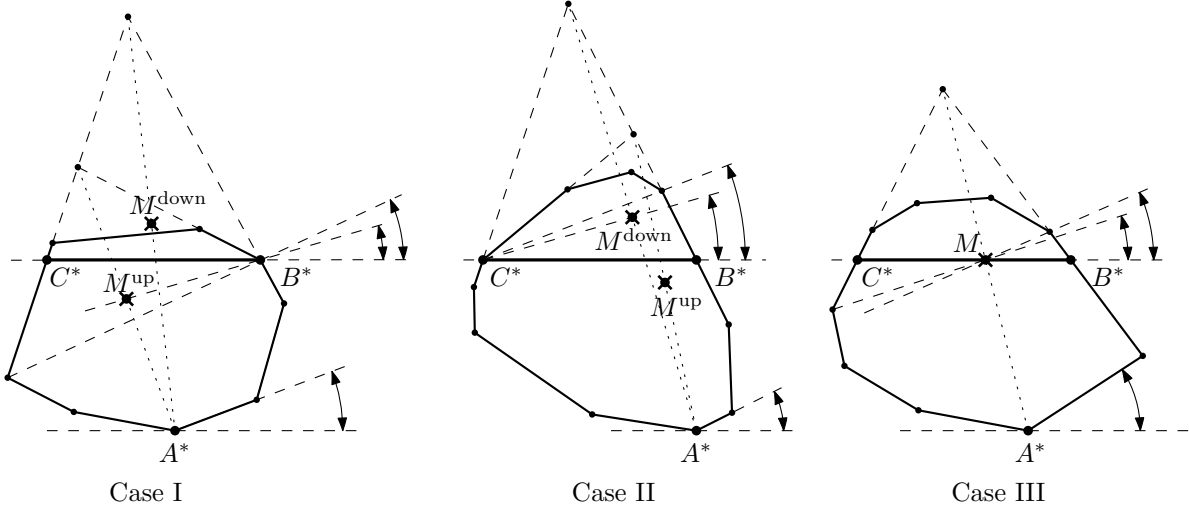
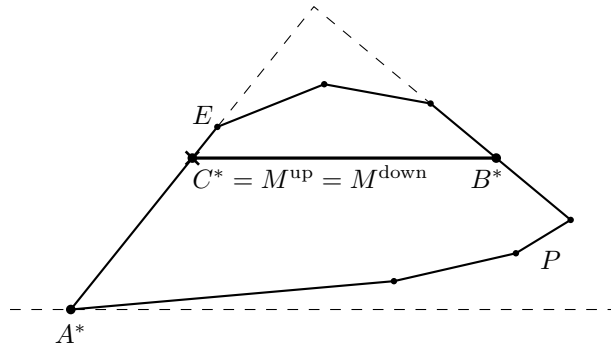


Figure 7: How the segment B^*C^* can rotate

- B262
- B263 In Case III, it may happen that the rotation center lies on an edge of P and hence coincides
 B264 with B^* or C^* , see Figure 8. Then this corner of the triangle remains stationary.



- B265 Figure 8: The pivot point M can lie on the boundary. (If this example is modified by shortening
 B266 the edge A^*E so that E coincides with C^* , then the pivot around which the rotation occurs is
 B267 still the point C^* , but the characteristic property $M^{\text{up}} = M^{\text{down}}$ of case III is lost, and we are
 B268 in Case II.)

B269 *Proof.* Consider a generic direction θ and the largest triangle according to Lemma 3. Two cases
 B270 can arise:

- If the two points B^* and C^* lie in the interior of two edges of P , then $M^{\text{up}} = M^{\text{down}}$, and
 B272 B^*C^* must go through this point; this condition does not change as long as B^* and C^*
 B273 remain in the interior of the edges on which they move.

B274 ¹⁰cf. [OAMB, Lemma 2]. See Appendix D for another proof.

B275 ¹¹cf. [ChMo, Lemma 3.1].

B276 • If one point, B^* or C^* , lies on a vertex of P and the other one lies in the interior of an
 B277 edge, then M^{up} and M^{down} are different, and they remain different provided that the point
 B278 B^* or C^* which lies at a vertex stays there. The optimality condition remains satisfied as
 B279 long as the segment B^*C^* does not cross M^{up} or M^{down} and as long as the moving point
 B280 stays on the same edge.

B281 There are degenerate situations which are not covered by these two cases: Both B^* and C^*
 B282 can lie on vertices of P ; or B^*C^* goes through a critical point M and a vertex of P that is
 B283 different from M . (Or both of these situations happen simultaneously.) However, there are only
 B284 finitely many potential pivot points and finitely many vertices. Thus, there are only finitely
 B285 many directions θ which are not covered by the two cases.

B286 We have therefore proved the first claim of the theorem: The open intervals with the same
 B287 combinatorial type cover all angles except for a finite set of breakpoints.

B288 Let us now look at these breakpoints. Figure 7 shows, for each case, the (at most) three
 B289 events that compete for terminating the motion or validity of the optimality conditions when
 B290 θ increases. One of the moving endpoints B^* or C^* might hit the endpoint of its edge, or the
 B291 rotating segment might hit one of the pivot points M^{up} or M^{down} . In addition, the point A^*
 B292 might jump to the next vertex. Of course, analogous events happen when θ is *decreased*.

B293 When θ reaches such a breakpoint, the optimality conditions continue to hold. This is
 B294 obvious if the rotating segment hits M^{up} or M^{down} . If one of the moving endpoints arrives at a
 B295 vertex, then M^{up} or M^{down} may jump. However, such a jump is always in the good direction
 B296 which makes the optimality conditions more liberal: M^{up} will jump to a lower position, and
 B297 M^{down} will jump higher. Thus, the rotating segment will remain optimal at the boundaries of
 B298 the intervals.

B299 The rotation induces a continuous counterclockwise motion of $B^*(\theta)$ and $C^*(\theta)$ inside each
 B300 interval. The only conceivably discontinuity is when B^*C^* coincides with the \mathbf{u} -extreme edge
 B301 of P , as in Figure 4b. However, in this case, it is easy to see that the segment will pivot around
 B302 B^* when θ is increased (see Lemma 7 below), and hence the motion of $B^*(\theta)$ is continuous also
 B303 here.

B304 Since the closed intervals $[\theta_i \dots \theta_{i+1}]$ overlap, the motion is continuous and monotone through-
 B305 out. Since the points $B^*(\theta)$ and $C^*(\theta)$ cannot overtake $A^*(\theta)$ or be overtaken by $A^*(\theta)$, they
 B306 have to make one complete turn.

B307 Finally, we bound number of breakpoints. We will justify below that at each breakpoint θ_i ,
 B308 one or more of the following happen:

- B309 a) A^* jumps.
- B310 b) B^* or C^* arrives at a vertex p_j as θ approaches θ_i from the left.
- B311 c) B^* or C^* moves away from a vertex p_j as θ increases from θ_i to the right.

B312 The breakpoints where A^* jumps are easy to count: There are exactly n of them. Each of the
 B313 four types of events where B^* or C^* arrives or moves away from a vertex p_j can happen at most
 B314 once per vertex, for a total of $4n$ events of these types. The extra $+1$ in the overall bound $5n + 1$
 B315 on the number of intervals is for the artificial cut at $0^\circ/360^\circ$.

B316 To justify the claim, consider an endpoint θ_i of an interval in the circular sweep. If A^* jumps,
 B317 or if B^* or C^* was moving and arrives at a vertex, the claim is fulfilled. The only remaining
 B318 case is when B^*C^* rotates around B^* at a polygon vertex (Case I) and hits the critical point
 B319 M^{up} , or symmetrically, when it rotates around C^* at a polygon vertex (Case II) and hits M^{down} .
 B320 Consider without loss of generality the latter case, see the middle picture of Figure 7. Then, if
 B321 θ is further increased, the segment B^*C^* will start to pivot around M^{down} and C^* will move
 B322 away from the vertex while B^* continues to move on its edge. This situation is optimal because
 B323 M^{down} does not change, and M^{up} jumps to M^{down} . (We are thus now in Case III. This
 B324 analysis is a special case of the Movement Rule that will be stated later in Lemma 7.) \square

B325 The bound $5n + 1$ is usually an overestimate. Even in a generic situation, an event of type
 B326 (b) and an event of type (c) can occur at the same breakpoint. Moreover, a breakpoint need
 B327 not manifest itself in the shape of the function $F(\theta)$. There are even polygons where $F(\theta)$ is
 B328 the constant function. One such example, from [BRS, Fig. 3], is the hexagon P with vertices
 B329 $(3, 0), (3, 3), (0, 3), (-1, \frac{5}{3}), (-1, 0), (0, -1)$.

B330 5 How the area changes when the direction is rotated

B331 **Lemma 6.** *In each closed interval $[\theta_i \dots \theta_{i+1}]$ where $B^*(\theta)$ and $C^*(\theta)$ lie on fixed edges, the area*
 B332 *function $F(\theta)$ has at most one local minimum.*

B333 *It has no local maximum in the interior of the interval, unless $F(\theta)$ is constant in that*
 B334 *interval.*

B335 *Proof.* The statement is clear if one endpoint is stationary (Cases I and II of Theorem 5): The
 B336 point A^* is also stationary, and the third point moves monotonically on an edge. Hence $F(\theta)$ is
 B337 either constant, or strictly increasing, or strictly decreasing.

B338 The more interesting case is Case III, when the segment rotates around M . First of all, we
 B339 note that $\text{area } A^*B^*C^* = \text{area } TC^*B^*$, see Figure 9a: Indeed, the segment B^*C^* bisects both
 B340 the triangle A^*TB^* and the triangle A^*TC^* , as is easily seen.

B341 We can thus look at the area of TC^*B^* . If we rotate the segment by a small amount $\Delta\theta$,
 B342 Figure 9b shows how the triangle area changes: It grows on the left side and shrinks on the
 B343 right side, by a triangular region in each case. We approximate these regions by circular sectors,
 B344 leaving an error of small order (the blue regions in the figure):

$$B345 \quad F(\theta + \Delta\theta) - F(\theta) = \Delta(\text{area } TBC) = \frac{1}{2} \cdot \Delta\theta \cdot (|C^*M|^2 - |B^*M|^2) + O(\Delta\theta^2)$$

B346 Letting $\Delta\theta \rightarrow 0$, one sees that the comparison between $|C^*M|$ and $|B^*M|$ decides about the sign
 B347 of the derivative of F . The stationary situation is attained when $|C^*M| = |B^*M|$. Figure 9c
 B348 shows that the unique segment B_0C_0 through M with this property can be obtained through
 B349 symmetry, by reflecting the rays TB^* and TC^* at M and intersecting them with the original
 B350 rays.

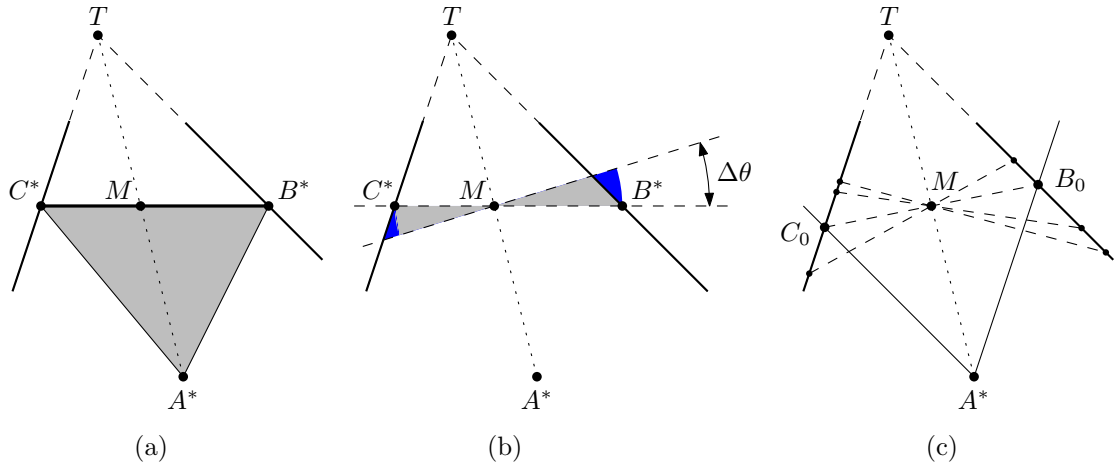
B351 As the segment B^*C^* rotates counterclockwise around M and the points B^*, C^* move on
 B352 the rays TB^* and TC^* , respectively, we initially have $|C^*M| < |B^*M|$, and $F(\theta)$ is strictly
 B353 decreasing, until we reach B_0C_0 . After this point, $|C^*M| > |B^*M|$ and $F(\theta)$ is strictly increasing.
 B354 □

B355 One might be tempted to prove Lemma 6 by showing that the pieces of $F(\theta)$ are convex
 B356 functions. However, this is not the case, at least in terms of the parameterization by the angle θ .
 B357 This can for example be observed (not very conspicuously) at the third piece from the left in
 B358 Figure 1.

B359 6 How the motion continues after a breakpoint

B360 There is an easy rule that tells how the motion continues when θ is increased. This rule works
 B361 irrespective of whether θ is at a breakpoint or not. Suppose we have determined the largest
 B362 anchored triangle $A^*(\theta)B^*(\theta)C^*(\theta)$, and we want to increase θ . Assume again for simplicity
 B363 that $\mathbf{u}(\theta)$ points vertically upwards. If A^* is not unique, we select the rightmost possibility, in
 B364 preparation for the increase of θ . Now we construct the intersection T^{forw} of the upward rays
 B365 through $e^{\text{forw}}(B^*)$ and $e^{\text{forw}}(C^*)$, and the *forward critical pivot point* $M^{\text{forw}} = (T^{\text{forw}} + A^*)/2$.

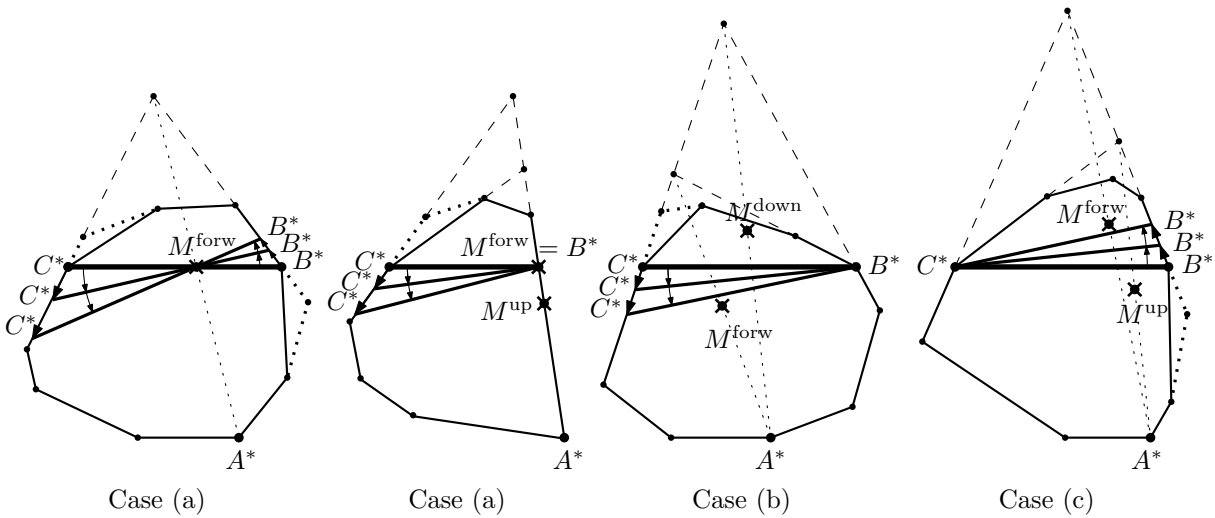
B366 **Lemma 7** (The Movement Rule). *If θ is increased, the segment B^*C^* moves as follows, see*
 B367 *Figure 10:*



B368 Figure 9: (a) $\text{area } A^*B^*C^* = \text{area } TC^*B^*$. (b) The area change under rotation of the segment
 B369 B^*C^* . (c) The balanced segment B_0C_0 with $|B_0M| = |C_0M|$.

- B370 a) If M^{forw} lies on B^*C^* , then B^*C^* will rotate around this point.
 B371 b) If M^{forw} lies below B^*C^* , then B^*C^* will rotate around B^* .
 B372 c) If M^{forw} lies above B^*C^* , then B^*C^* will rotate around C^* . This includes the case that
 B373 M^{forw} does not exist because the upward rays through $e^{\text{forw}}(B^*)$ and $e^{\text{forw}}(C^*)$ don't meet.

B374 This rule is consistent with the tendency that B^*C^* wants to get (or stay) close to M^{forw} .



B375 Figure 10: The pivot point around which the segment B^*C^* rotates. Case (a): an interior point
 B376 or B^* or C^* (not shown); Case (b): B^* ; Case (c): C^* . The labels M^{forw} , M^{up} , M^{down} refer to
 B377 the situation before the motion starts. In some cases, it does not matter whether B^* or C^* lies
 B378 on a vertex or not. This is indicated by dotted variations of the polygon P .

B379 *Proof.* We prove that the described movement maintains optimality. If B^*C^* rotates around
 B380 B^* , it can be for two reasons: Either we are in Case (b), or M^{forw} coincides with B^* in Case (a).
 B381 In both cases, C^* will be interior to $e^{\text{forw}}(C^*)$ after the rotation starts, $e^{\text{back}}(C^*)$ will coincide
 B382 with this edge $e^{\text{forw}}(C^*)$, and M^{forw} becomes M^{up} . Thus, M^{up} will be on B^*C^* , in Case (a),
 B383 or below B^*C^* , in Case (b). M^{down} stays the same as before. Since B^*C^* was assumed to be

B384 optimal, M^{down} lies on or above B^*C^* , and it remains so since B^*C^* rotates downwards. Thus
 B385 the optimality conditions are preserved.

B386 If B^*C^* rotates around C^* , the argument holds *mutatis mutandis*.

B387 Finally, if M^{forw} lies in the interior of B^*C^* in Case (a) and B^*C^* rotates around this point,
 B388 then $M^{\text{up}} = M^{\text{down}} = M^{\text{forw}}$ after the rotation starts, and optimality is clear. \square

B389 We mention that the Movement Rule gives the right movement when B^*C^* coincides with
 B390 the \mathbf{u} -extreme edge of P : Then $T^{\text{forw}} = C^*$, and M^{forw} lies below B^*C^* . Hence the segment
 B391 will rotate around B^* .

B392 7 A linear-time algorithm for the Circular Sweep

B393 It is straightforward to distill a linear-time algorithm for finding the largest anchored triangles
 B394 for all directions θ from Lemmas 1 and 16:

B395 We first compute the largest anchored triangle $A^*(\theta_0)B^*(\theta_0)C^*(\theta_0)$ for the starting direc-
 B396 tion $\theta_0 = 0^\circ$. This triangle can be found in $O(\log^2 n)$ time¹² by nested binary search on the left
 B397 and right boundary of P for the optimal height h , using the local optimality criteria of Lemma 3.
 B398 Since we are going to spend linear time anyway, and since we need to do this only once for the
 B399 initialization, we can instead perform a simple linear scan in linear time.¹³

B400 We increase θ continuously to 360° and move the three corners A^*, B^*, C^* along.¹⁴ We imagine
 B401 this as a continuous process. We have to watch for three types of events, as described in the
 B402 proof of Theorem 5, see Figure 7:

- B403 1. A^* jumps to the next corner.
- B404 2. A sliding corner B^* or C^* arrives at a vertex.
- B405 3. The segment B^*C^* hits a critical point M^{up} or M^{down} .

B406 Whenever this happens, we are at a breakpoint, and we determine how the motion continues
 B407 with the help of the Movement Rule of Lemma 7. By Theorem 5.iii, there are $O(n)$ events, and
 B408 an event can be processed in $O(1)$ time. Thus, the overall effort is linear.

B409 If we are looking for a largest inscribed triangle, Lemma 6 implies that it is sufficient to
 B410 evaluate the area at the breakpoints and take the maximum. If we are looking for a smallest
 B411 circumscribed triangle, we additionally have to consider the possibility of an interior local mini-
 B412 mum, which is constructed according to Figure 9c for those intervals where B^*C^* rotates around
 B413 an interior point M .¹⁵

B414 Thus, we have achieved a linear-time algorithm, both for the largest inscribed triangle and
 B415 the smallest circumscribed triangle. As we will see in the subsequent sections, there are special
 B416 properties of the two problems that allow the algorithm to be simplified.

B417 We can even construct the complete function $F(\theta)$, as in Figure 1. It is a continuous piecewise
 B418 smooth function with at most $5n + 1$ pieces. It is not hard to see from Figure 9b that each piece
 B419 can be written in the form $F(\theta) = \alpha + \beta_1 \tan(\theta + \gamma_1) + \beta_2 \tan(\theta + \gamma_2)$ for some constants
 B420 $\alpha, \beta_1, \gamma_1, \beta_2, \gamma_2$.

B421 ¹²See [KILa, Section 2]. Footnote 21 sketches a faster method with only $O(\log n)$ runtime.

B422 ¹³We can either search from bottom to top or from top to bottom. A different initialization procedure, which
 B423 searches B^* and C^* by moving a tentative point B^* from bottom to top while advancing C^* downwards from top
 B424 to bottom, is described in Section 9, see Footnote 23.

B425 ¹⁴It is actually sufficient to sweep up to 180° : The largest or smallest triangle ABC will be discovered whenever
 B426 $\mathbf{u}(\theta)$ is the outer normal of one of the three sides of ABC .

B427 ¹⁵In the beginning of Section 9, we will see that this extra effort for looking in the interior of intervals can be
 B428 saved.

8 Speed-up for the largest inscribed triangle

B429 It is well-known that the largest triangle has its corners at vertices of P :

B430 **Lemma 8.** *The largest inscribed triangle ABC in a polygon P can be found among the triangles*
 B431 *whose corners A, B, C are among the vertices of P .*

B432 *Proof.* If a corner lies in the interior of an edge, then it can slide to one of the two endvertices
 B433 of this edge without decreasing the area, keeping the other two corners fixed. \square

B434 Keeping this property in mind, we restrict our attention to points $A(\theta), B(\theta), C(\theta)$ that lie
 B435 on vertices of P . We can formulate the following

B436 *Skipping Principle.* When, at any time during the Circular Sweep, it becomes known
 B437 that $B^*(\theta)$ lies on a point B in the interior of an edge $p_i p_{i+1}$ of the polygon, or that it
 B438 must lie ahead of such a point B , then it is not necessary to increase θ continuously.
 B439 We can immediately advance B^* to the forward endpoint p_{i+1} of this edge, and
 B440 adjust θ accordingly.

B441 The same statement holds for C^* .

B442 8.1 The Skipping Algorithm

B443 This results in the algorithm shown in Figure 11. The algorithm maintains three points A, B, C
 B444 that move counterclockwise through the vertices of P . When we say we *advance* A or B or C we
 B445 mean that we move it to the next vertex of P . The next vertex after A is denoted by $next(A)$.
 B446 The direction θ does not explicitly appear in the algorithm but we can think of $\mathbf{u}(\theta)$ as attached
 B447 to BC as its normal vector.

Compute $A^*(\theta_0), B^*(\theta_0),$ and $C^*(\theta_0)$ for $\theta_0 = 0^\circ$. (Initialization)
 set A to the forward endpoint of $e^{\text{back}}(A^*(\theta_0))$
 set B to the forward endpoint of $e^{\text{back}}(B^*(\theta_0))$
 set C to the forward endpoint of $e^{\text{back}}(C^*(\theta_0))$
 $maxarea := 0$

(*) **while** B is not to the left of C : (θ has not completed a half-turn)

(i) **if** $area\ next(A)BC \geq area\ ABC$:
 advance A . (Move towards the extreme point $A^*(\theta)$ in direction $-\mathbf{u}(\theta)$)

(ii) **else if** decreasing h would increase the area:
 advance C . (Move towards $C^*(\theta)$)

(iii) **else if** increasing h is possible and would increase the area:
 advance B . (Move towards $B^*(\theta)$)

else: (Now $BC = B^*(\theta)C^*(\theta)$, and ABC is a candidate for the largest triangle.)
 $maxarea := \max(maxarea, area\ ABC)$

(iv) Determine how the edge B^*C^* will rotate when θ continues to increase.
 It rotates either
 around B^* or
 around C^* or
 around a critical pivot point M in the interior of the edge B^*C^* .
 Accordingly, either C^* , or B^* , or both points move.
 Advance the corresponding point C , or B , or both B and C

B448 Figure 11: The Skipping Algorithm for the largest inscribed triangle

B449 The initialization makes sure that A lies at a vertex, and it advances B and C to the next
 B450 vertex if $B^*(\theta_0)$ or $C^*(\theta_0)$ lies in the middle of an edge, following the Skipping Principle.

B451 The test (i) ensures that the rest of the loop is not entered before A is at the point $A^*(\theta)$
 B452 for the current direction θ . In case of a tie, we advance A in order to be prepared for increasing
 B453 θ in step (iv).

B454 The advancements in steps (ii)–(iv) are justified by the Skipping Principle. The conditions
 B455 in steps (ii) and (iii) are checked according to the Improvement Test (conditions (1)–(2)) and the
 B456 criteria (a) and (b) of Lemma 3. The test in step (iv) is carried out according to the Movement
 B457 Rule (Lemma 7).

B458 The termination condition (*) will be discussed in Section 8.3.

B459 8.2 Simplifying the test: Jin’s Algorithm

B460 The tests (ii)–(iv) can be subsumed in one simple common test:

```
B461   Construct the point  $M^{\text{forw}}$ 
B462   if  $M^{\text{forw}}$  lies below  $BC$ :
B463       advance  $C$ 
B464   else if  $M^{\text{forw}}$  lies on or above  $BC$  or  $M^{\text{forw}}$  does not exist:
B465       advance  $B$ 
```

B466 Indeed, by construction, M^{forw} lies higher than M^{up} and lower than M^{down} . Thus, if the test (ii)
 B467 succeeds because M^{down} lies below BC , then M^{forw} lies below BC and the simplified algorithm
 B468 will do the right thing. If the test (iii) succeeds because M^{up} lies on or above BC , the analogous
 B469 argument leads to the same conclusion. (If M^{up} does not exist then M^{forw} does not exist.)

B470 Finally, let us consider the test (iv). It is carried out when $BC = B^*C^*$, and hence the Move-
 B471 ment Rule (Lemma 7) applies. If M^{forw} does not lie on B^*C^* (Cases (b) and (c) of Lemma 7),
 B472 the segment rotates around one endpoint, and the other endpoint can be advanced. The simpli-
 B473 fied algorithm makes the right choice. Finally, if M^{forw} lies on B^*C^* , the simplified algorithm
 B474 always advances B , whereas the original Skipping Algorithm would sometimes advance C or
 B475 both points. If M^{forw} lies in the interior of B^*C^* , the original Skipping Algorithm advances
 B476 both points. Here, the simplified algorithm behaves differently. However, advancing only B is
 B477 still correct since it is justified by the Skipping Principle. (It is simpler to avoid an extra test
 B478 and miss a few opportunities of advancing a point.)

B479 The only case when there would be a discrepancy between the Skipping Algorithm and the
 B480 simplified test is when $M^{\text{forw}} = B^*$ and therefore C should be advanced, see the second example
 B481 in Figure 10. However, M^{forw} can coincide with B^* only if the edge $e^{\text{forw}}(B^*)$ extends all the
 B482 way down to A^* . Since $B^* = B$ is a vertex of P , this case is excluded.

B483 The whole loop, together with the advancement of A , becomes extremely simple:

```
B484   while  $B$  is not to the left of  $C$ :
B485       while  $\text{area next}(A)BC \geq \text{area } ABC$ :
B486           advance  $A$ 
B487            $\text{maxarea} := \max(\text{maxarea}, \text{area } ABC)$ 
B488       if  $M^{\text{forw}}$  exists and lies below  $BC$ :
B489           advance  $C$ 
B490       else:
B491           advance  $B$ 
```

B492 Since we don’t distinguish whether $BC = B^*C^*$, we simply take all triangles ABC that we
 B493 encounter after the loop (i) as candidates for the largest triangle.¹⁶ We call this *Jin’s Algorithm*.

B494 ¹⁶On a superficial level, the algorithm resembles the incorrect algorithm of Dobkin and Snyder [DS]. However,
 B495 that algorithm controls the advancement of B and C by a different criterion, namely the comparison of areas.

B496 The algorithm for the largest inscribed triangle as described in Jin [Jin] uses a different initial-
 B497 ization¹⁷ and termination condition, but apart from that, it differs only in minor details.¹⁸ Jin
 B498 did not derive his algorithm as a simplification of the circular sweep over all anchored triangles,
 B499 but with a different approach, the *Rotate-and-Kill* method.

B500 A nice feature of this algorithm, besides a potential speedup, is that the only points A , B ,
 B501 and C that are ever considered are vertices of the polygon. Even in the initialization step, when
 B502 B^* and C^* are found by scanning the left and right side of P simultaneously, it is never necessary
 B503 to explicitly handle any boundary points B^* and C^* that are not vertices. All that is necessary
 B504 is a comparison of critical points M with vertices.

B505 8.3 Correctness, termination, and running time

B506 The Skipping Algorithm starts with $\theta = 0^\circ$ and rotates the direction until the condition $(*)$
 B507 indicates termination. This happens when the normal direction of BC falls in the range $180^\circ <$
 B508 $\theta < 360^\circ$. The Skipping Algorithm is guaranteed to visit at least all triangles $A^*(\theta)B^*(\theta)C^*(\theta)$
 B509 for which both $B^*(\theta)$ and $C^*(\theta)$ lie at vertices of P (in addition to $A^*(\theta)$). The largest inscribed
 B510 triangle has these properties, and, like every triangle, it has some normal $\mathbf{u}(\theta)$ in the range
 B511 $0^\circ \leq \theta < 180^\circ$. Thus, it is ensured that the largest inscribed triangle is found before the
 B512 algorithm terminates.

B513 The termination argument is a little subtle because the three points A, B, C are not always
 B514 distinct.

B515 **Lemma 9.** *Assume that P has at least 3 vertices. In the Skipping Algorithm, both in the original*
 B516 *and the simplified version, collisions between the points A, B, C are subject to the following*
 B517 *constraints:*

- B518 a) *The points B and C are always distinct.*
- B519 b) *As the points are advanced, C can catch up with A , and A can catch up with B , but no point*
 B520 *overtakes another point.*
- B521 c) *Consequently, the points A, B, C are always in counterclockwise order whenever they are*
 B522 *distinct.*

B523 *Proof.* We have seen after Lemma 7 that B is not advanced when $C = \text{next}(B)$, because this is
 B524 the case when BC is the \mathbf{u} -extreme edge. It is possible that C catches up with A (even right
 B525 after initialization), but then A will immediately advance. So C cannot overtake A .

B526 The point A can only catch up with B if $B = \text{next}(C)$. This can indeed happen, for example
 B527 when P is a triangle. In this situation, the next step will advance B . Thus, B and C remain
 B528 always distinct, and A cannot overtake B .

B529 In the original version of the Skipping Algorithm, there is a case when both B and C move
 B530 simultaneously, but then the only collision that can happen is that C runs into A , and this case
 B531 has been treated above. □

B532 Since B and C are always distinct, the segment BC has a well-defined direction.

B533 ¹⁷Jin initializes his algorithm with a “3-stable” triangle. One can easily see that a 3-stable triangle is the largest
 B534 anchored triangle for all three directions to which it is anchored. Jin shows how to find such a triangle in linear
 B535 time by a simple algorithm, which considers only triangles with vertices from the polygon [Jin, Section 2].

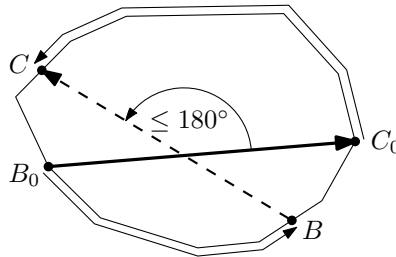
B536 ¹⁸The main difference is that the algorithm in [Jin] does not advance A in case of equality. Our choice of
 B537 advancing A was necessary for the original Circular Sweep Algorithm of Section 7, but one can easily check that
 B538 in the present simplified algorithm, it makes no difference whether we advance A or not in case of ties. The other
 B539 difference is that the test is not expressed in term of the critical point M^{forw} but in another, equivalent way, see
 B540 Appendix B.2.2.

B541
B542

Lemma 10. *The counterclockwise change of direction of the segment BC in one step of the algorithm is less than 180° .*

B543
B544
B545
B546
B547
B548

Proof. The points B and C can advance only one vertex at a time (perhaps simultaneously, in the original Skipping Algorithm). Now, consider moving two points B and C forward on the boundary of a convex region from some starting position B_0C_0 , without B moving past C_0 or C moving past B_0 , see Figure 12. Then one can turn the segment BC by at most 180° , and the only way to reach 180° is for B and C to swap places, but this is impossible in one step in a polygon with more than 2 vertices. \square



B549

Figure 12: How much BC can rotate in one step

B550
B551
B552
B553
B554

So we know that the direction θ increases from the initial value 0° in steps less than 180° . Thus it cannot jump over the terminating interval $180^\circ < \theta < 360^\circ$ in one step. Consequently, the total counterclockwise turn of the segment BC is less than 360° .

Termination in linear time is now guaranteed by the fact that each loop iteration advances one or several of the points A, B, C , and the points cannot overtake each other. \square

B555

Exercise. 1. True or false:

B556
B557
B558
B559

- The loop can be stopped already as soon as A is to the right of B ,
 - (a) because the sequence of triangles starts repeating from this point, with rotated labels A, B, C ;
 - (b) for a different reason.

B560
B561

- 2. In case this improved termination condition works: At what point in the algorithm should it be tested?

9 Speed-up for the smallest circumscribed triangle

B562
B563

We will now specialize the Circular Sweep algorithm of Section 7 to smallest circumscribed triangles. The following basic observation allows to simplify the algorithm in this case.

Lemma 11. *There is a smallest circumscribed triangle that touches a polygon edge.¹⁹*

B564
B565
B566

Proof. The smallest circumscribed triangle is anchored at some direction \mathbf{u} . According to Lemma 4.ii, there is a smallest circumscribed triangle anchored at that direction with the claimed property. \square

B567
B568

A circumscribed triangle that touches a polygon edge is anchored at the outer normal direction of that edge. Thus, *it suffices to look at $F(\theta)$ for those breakpoints which are inner normals*

B569
B570
B571

¹⁹In fact, every smallest circumscribed triangle has this property. This follows from [KILa, Lemma 1.3], see also [KILa, Theorem 2.1.iv]. Also, there is a smallest circumscribed triangle that touches at least two polygon edges, cf. [OAMB, Lemma 1].

B572 of polygon edges (where A^* jumps). In particular, this implies that it is not necessary to look
 B573 at the local minima in the interior of the intervals: The same minima will also be discovered at
 B574 breakpoints.

B575 One can use this observation to shortcut the sweep more aggressively. In the algorithm of
 B576 O'Rourke, Aggarwal, Maddila, and Baldwin [OAMB], θ jumps from one inner normal direction of
 B577 P to the next. Like in the Skipping Algorithm in Figure 11, two points B and C are maintained.
 B578 After increasing θ , we will approach $B^*(\theta)$ and $C^*(\theta)$ step by step by moving either B or C to
 B579 the next vertex.

B580 A typical situation is shown in Figure 13a. We again assume w. l. o. g. that \mathbf{u} points vertically
 B581 upward. We have the points $B = B^*(\theta^{\text{old}})$ and $C = C^*(\theta^{\text{old}})$ from the previous direction θ^{old} ,
 B582 and we have advanced θ to the next edge, on which A^* now lies. By Theorem 5.ii, we know that
 B583 the points $B^* = B^*(\theta)$ and $C^* = C^*(\theta)$ can only lie ahead of B and C . Statements 1 and 2 of
 B584 the following lemma allows us to advance B or C while maintaining this property.

B585 The boundary of P has a *left side* and a *right side*, relative to the current direction \mathbf{u} . (Edges
 B586 perpendicular to \mathbf{u} belong to neither side.) We denote by $h(X)$ the *height* of the point X over
 B587 A^* in direction \mathbf{u} .

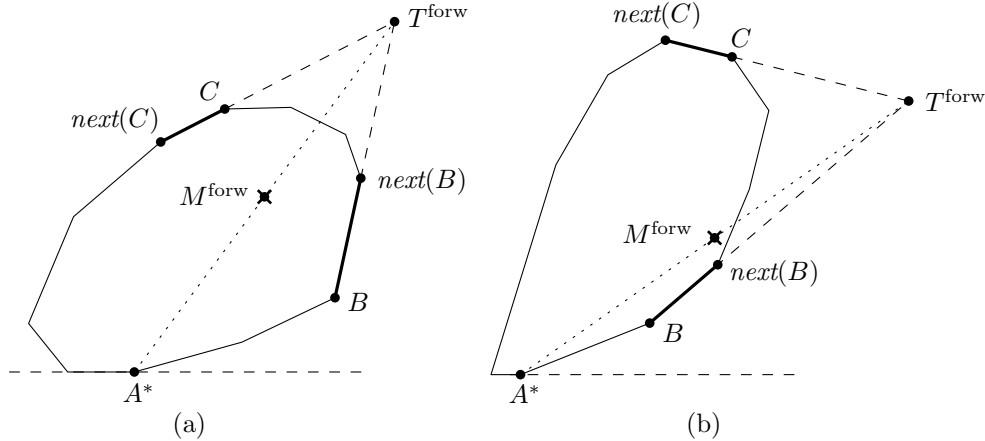
B588 **Lemma 12.** ²⁰ Let $(B, \text{next}(B))$ be an edge on the right side and let $(C, \text{next}(C))$ be an edge on
 B589 the left side of a convex polygon P . Let M^{forw} be the critical point computed from these edges,
 B590 as illustrated in Figure 13a.

B591 1. If $h(M^{\text{forw}}) \leq h(\text{next}(C))$ and $h(\text{next}(C)) \geq h(B)$, then

B592
$$h(B^*) = h(C^*) \leq h(\text{next}(C)).$$

B593 2. If $h(M^{\text{forw}}) \geq h(\text{next}(B))$ or M^{forw} does not exist, and $h(\text{next}(B)) \leq h(C)$, then

B594
$$h(B^*) = h(C^*) \geq h(\text{next}(B)).$$



B595 Figure 13: (a) The criterion for advancing either B or C . (b) The situation when C is not on
 B596 the left side.

B597 *Proof.* 1. We apply the Improvement Test to the upward direction at height $h(\text{next}(C))$.
 B598 The point M^{up} is determined by the ray through $(C, \text{next}(C))$, and the ray through either
 B599 $(B, \text{next}(B))$ or through a higher edge. Since the edges bend inwards when going from $(B, \text{next}(B))$

B600 ²⁰[OAMB, Lemmas 3 and 4] obtain the same conclusions under the stronger assumption that $h(\text{next}(C)) >$
 B601 $h(\text{next}(B))$.

B602 to a higher edge, $h(M^{\text{up}}) \leq h(M^{\text{forw}})$. With the assumption $h(M^{\text{forw}}) \leq h(\text{next}(C))$ we get
 B603 $h(M^{\text{up}}) \leq h(\text{next}(C))$, which implies that B^*C^* cannot lie above $\text{next}(C)$.

B604 2. The second statement is completely analogous. We apply the Improvement Test to the
 B605 downward direction at height $h(\text{next}(B))$. The point M^{down} is determined by the ray through
 B606 $(B, \text{next}(B))$, and the ray through either $(C, \text{next}(C))$ or through a lower edge. Since the edges
 B607 bend outwards when going from $(C, \text{next}(C))$ to a lower edge, $h(M^{\text{down}}) \geq h(M^{\text{forw}})$ if M^{down}
 B608 exists, and if M^{forw} does not exist, the M^{down} does not exist. With the assumption $h(M^{\text{forw}}) \geq$
 B609 $h(\text{next}(B))$ we get $h(M^{\text{down}}) \geq h(\text{next}(B))$ if M^{down} exists at all, which implies that B^*C^*
 B610 cannot lie below $\text{next}(B)$. □

(i) $B := p_1$ and $C := p_2$
 $\text{minarea} := \infty$
for $i := 1 \dots n$:
 let \mathbf{u} be the inner normal of the edge $p_{i-1}p_i$, and set $A^* := p_i$
 (ii) **while** $h(\text{next}(C)) \geq h(C)$: (Ensure that C lies on the left side)
 advance C
 loop
 (iii) compute the critical point $M^{\text{forw}} = (T^{\text{forw}} + A^*)/2$ from the intersection T^{forw}
 of the forward extension of the edge $(B, \text{next}(B))$
 and the backward extension of the edge $(C, \text{next}(C))$.
 (iv) **if** $h(M^{\text{forw}}) \leq h(\text{next}(C))$:
 if $h(\text{next}(C)) \geq h(B)$:
 advance C downwards to $\text{next}(C)$
 else: exit loop
 (v) **else if** $h(M^{\text{forw}}) \geq h(\text{next}(B))$, or M^{forw} does not exist:
 if $h(\text{next}(B)) \leq h(C)$:
 advance B upwards to $\text{next}(B)$
 else: exit loop
 else: exit loop
 We now know the edges $(B, \text{next}(B))$ and $(C, \text{next}(C))$ on which B^* and C^* lie.
 Construct the horizontal segment B^*C^* between these edges as follows:
 (vi) **if** $h(M^{\text{forw}}) \leq h(B)$:
 $B^* = B$, and C^* lies on $(C, \text{next}(C))$ at the same height as B
 (vii) **else if** $h(M^{\text{forw}}) \geq h(C)$ or M^{forw} does not exist:
 $C^* = C$, and B^* lies on $(B, \text{next}(B))$ at the same height as C
 (viii) **else**:
 B^*C^* lies at the height of M^{forw}
 $\text{minarea} := \min(\text{minarea}, 4 \cdot \text{area } A^*B^*C^*)$.

B611 Figure 14: The linear-time algorithm specialized for the smallest circumscribed triangle

B612 This lemma is important because it allows to draw conclusions about the height of B^*C^*
 B613 from two points B and C which are not at the same height.²¹ It is the basis for the algorithm

B614 ²¹Lemma 12 can be used to compute a largest anchored triangle by the prune-and-search technique in $O(\log n)$
 B615 time, as opposed to the nested binary search mentioned at the beginning of Section 7, which requires $O(\log^2 n)$
 B616 time. Lemma 12 is geared towards the case that $(C, \text{next}(C))$ is higher than $(B, \text{next}(B))$. It has a mirror-
 B617 symmetric version in which the roles of $B, \text{next}(B), C, \text{next}(C)$ are swapped with $\text{next}(C), C, \text{next}(B), B$, and
 B618 which applies in the opposite situation.

B619 We maintain a chain of *left candidate edges* and a chain of *right candidate edges* on which the true points B^*
 B620 and C^* can lie. Initially, all left and right edges are candidates. We pick the median B and C from each chain and
 B621 compute M^{forw} for the edges $(B, \text{next}(B))$ and $(C, \text{next}(C))$. If the height ranges of $(B, \text{next}(B))$ and $(C, \text{next}(C))$

B622 shown in Figure 14. There is an outer loop that cycles through all inner normal directions \mathbf{u} of
 B623 the edges and records the largest area. In the main inner loop (iii)–(v), the algorithm looks for
 B624 the edges $(B, \text{next}(B))$ and $(C, \text{next}(C))$ that contain B^* and C^* . For this purpose, B and C
 B625 are advanced towards B^* and C^* , maintaining the invariant that *the correct segment B^*C^* is*
 B626 *sandwiched between B and C :*

$$B627 \quad h(B) \leq h(B^*) = h(C^*) \leq h(C) \quad (3)$$

B628 Let us discuss how this invariant is maintained, ignoring for the time being the question of
 B629 termination of the inner loop and the computation of B^*C^* in the second part (vi)–(viii). After
 B630 the tests (iv) and (v), the advancement of B and C is justified by Lemma 12, provided that B
 B631 lies on the right side and C lies on the left side. It can happen that C starts out on the right
 B632 side after the direction \mathbf{u} has been advanced, as shown in Figure 13b. The loop (ii) ensures that
 B633 C is moved over to the left side before the main loop starts.²² Another potentially dangerous
 B634 situation is that B lies on the bottom horizontal edge, to the left of A^* . In this case, T^{forw} does
 B635 not exist, and the algorithm automatically advances B to coincide with A^* , which is the right
 B636 action. So, this special case is resolved without requiring special treatment.

B637 When the point A^* together with the normal direction \mathbf{u} is advanced, we leave the points
 B638 B and C as they are. We don't initialize them to the previous points B^* and C^* , as suggested
 B639 in our first informal description of the algorithm. The invariant is maintained according to the
 B640 monotonic movement of $B^*(\theta)$ and $C^*(\theta)$ (Theorem 5.ii) *unless* B or C are on the wrong side
 B641 after the increase of θ . In this case, as we have seen, the algorithm will first move B and C to
 B642 the first vertex on the correct side, either explicitly in (ii), for C , or implicitly, for B , and the
 B643 invariant is trivially reestablished at this point.

B644 To *initialize* the process for the first direction \mathbf{u} , we start with B at the lowest vertex on the
 B645 right side and C at the highest vertex on the left side. Then the invariant holds trivially. In
 B646 line (i), we have set C to the vertex after B , and the loop (ii) ensures that C crawls over to the
 B647 top of the left side.²³

B648 It is easy to argue that the inner loop must *terminate*: We have proved that we maintain
 B649 the invariant (3), and in particular, the relation $h(B) \leq h(C)$. Since B moves upwards and C
 B650 moves downwards from vertex to vertex, the loop cannot run forever.

B651 Let us now turn to the construction of B^*C^* in (vi)–(viii). The following auxiliary lemma
 B652 will be used to justify the cases (vi) and (vii). In contrast to Lemma 12, this lemma applies
 B653 when the vertical ranges of the edges $(B, \text{next}(B))$ and $(C, \text{next}(C))$ overlap.

B654 **Lemma 13.** *In addition to the assumptions of Lemma 12, we assume the invariant (3).*

B655 don't overlap, then Lemma 12 or its symmetric counterpart is guaranteed to give a conclusion about the relative
 B656 height of B^* and C^* with respect to at least one of the four involved vertices. Thus, we can discard half of the
 B657 edges of either the left chain or the right chain, give or take one or two edges for rounding effects.

B658 If the height ranges of $(B, \text{next}(B))$ and $(C, \text{next}(C))$ overlap, we can perform the standard Improvement Test
 B659 for one of the vertices that lie in the overlapping interval, and discard half of the edges from *both* chains.

B660 One chain is reduced to a constant number of edges after $O(\log n)$ such tests, and the search can be finished
 B661 with standard binary search in $O(\log n)$ time.

B662 ²²The loop (ii) can actually be omitted because the second loop (iii)–(v) will do the right thing on its own:
 B663 Our definition of M^{forw} from the *backward* extension of the edge $(C, \text{next}(C))$ in line (iii) is appropriate for this
 B664 situation. This definition is consistent with our convention of using the “upward” ray extending $(C, \text{next}(C))$
 B665 when C lies on the left side, and it is also consistent with the way how T^{forw} is conveniently computed, see
 B666 Appendix B.2.1. In Figure 13b, we see that, when C is on the right side, T^{forw} is below C and $\text{next}(C)$, and
 B667 so is M^{forw} . Also, since B and C are on the right side, $h(\text{next}(C)) \geq h(C) \geq h(B)$, and thus the algorithm
 B668 advances C . (For this case, the description of advancing C “downwards” in (iv) is not appropriate.) The same
 B669 happens in the boundary case when the edge $(C, \text{next}(C))$ is a horizontal \mathbf{u} -extreme edge.

B670 ²³This initialization together with a single iteration of the outer loop gives another way of computing a largest
 B671 anchored triangle from scratch in linear time, and thus for initializing any of the other derivatives of the Circular
 B672 Sweep algorithm.

B673 1. If $h(M^{\text{forw}}) \leq h(B)$ and $h(\text{next}(C)) \leq h(B)$, then

B674
$$h(B^*) = h(C^*) = h(B)$$

B675 2. If $h(M^{\text{forw}}) \geq h(C)$ or M^{forw} does not exist, and $h(\text{next}(B)) \geq h(C)$, then

B676
$$h(B^*) = h(C^*) = h(C).$$

B677 The proof will be given below.

B678 There are three ways of terminating the inner loop. Let us first consider the exit when
B679 neither of the conditions (iv) and (v) hold:

B680
$$h(\text{next}(C)) < h(M^{\text{forw}}) < h(\text{next}(B)) \tag{4}$$

B681 The easiest case is case (viii), when $h(B) < h(M^{\text{forw}}) < h(C)$: then both points B^*C^* at height
B682 $h(M^{\text{forw}})$ lie in the interior of the respective edges $(B, \text{next}(B))$ and $(C, \text{next}(C))$. The critical
B683 points $M^{\text{up}} = M^{\text{down}} = M^{\text{forw}}$ coincide, and the optimality condition of Lemma 3 is fulfilled.

B684 In case (vi), $h(M^{\text{forw}}) \leq h(B)$, and this together with (4) implies the second assumption
B685 of Lemma 13.1. In case (vii), $h(M^{\text{forw}}) \geq h(C)$, and this together with (4) implies the second
B686 assumption of Lemma 13.2. In either case, Lemma 13 justifies the decision of the algorithm.

B687 If the exit of the loop was through (iv), then

B688
$$h(M^{\text{forw}}) \leq h(\text{next}(C)) < h(B).$$

B689 The algorithm will thus take the branch (vi), and this is justified by Lemma 13.1.

B690 If the exit of the loop was through (v), then

B691
$$h(M^{\text{forw}}) \geq h(\text{next}(B))$$

B692 if M^{forw} exists, and

B693
$$h(\text{next}(B)) > h(C).$$

B694 The algorithm will thus take the branch (vii), and this is justified by Lemma 13.2.

B695 To conclude the correctness proof of the algorithm, we supply the easy proof of Lemma 13:

B696 *Proof of Lemma 13.* 1. Let us tentatively put B^*C^* at the height of $h(B)$ and see why this
B697 is the correct solution. If $h(B) = h(C)$, the invariant (3) leaves no other choice for B^*C^* .
B698 Otherwise, $h(C) > h(B)$, and then the critical point M^{up} at the height of B is determined by
B699 the same edges as M^{forw} . Thus, $h(M^{\text{up}}) = h(M^{\text{forw}}) \leq h(B)$. Then the optimality condition of
B700 Lemma 3b tells us that the optimal segment B^*C^* does not lie above B . By the invariant, we
B701 know that B^*C^* cannot lie below B . Thus, B^*C^* must go through B .

B702 2. The second statement is analogous. □

B703 It is easy to see that the algorithm takes only linear time. There are n iterations of the outer
B704 loop, advancing A^* one vertex at a time. Each iteration of an inner loop advances B or C , but
B705 B and C cannot overtake A^* .

B706 This algorithm shares the nice feature with Jin's Algorithm of Section 8.2 that the points
B707 A^* , B , and C range only over vertices.

B708 The shortcut in this section is similar in spirit to the shortcut introduced in Section 8 for
B709 the largest inscribed triangle by way of the Skipping Principle. The crucial difference is that, in
B710 Section 8, we advance B and C and let \mathbf{u} follow. Here, we advance the direction \mathbf{u} , and B and
B711 C have to catch up.

A Literature

B713 This note gives a self-contained development of linear-time algorithms for largest inscribed and
 B714 the smallest circumscribed triangle, starting from scratch. The essential ideas and inspirations
 B715 have been taken from the literature, but I have tried to streamline the presentation for simplicity.
 B716 A distinguishing feature of my treatment is the central role that is given to the critical pivot
 B717 point M . As discussed in Appendix B.2.2, the same optimality condition (Lemma 3) appears
 B718 in various other guises in the literature. I hope that my presentation may contribute to the
 B719 clarification of the ideas underlying the algorithms. I have sprinkled the text with footnotes
 B720 that acknowledge sources or clarify clashes of terminology.

B721 I give a brief account of the relevant literature in chronological order, together with the
 B722 publication dates.

- B723 • Dobkin and Snyder [DS] in 1979 were the first to propose a linear-time algorithm for the
 B724 largest inscribed triangle. In 2017, this algorithm found to be wrong, see below.
- B725 • In 1985, Klee and Laskowski [KLa] developed an algorithm for computing the smallest
 B726 circumscribed triangle in $O(n \log^2 n)$ time.²⁴
- B727 • Building on this work, O’Rourke, Aggarwal, Maddila, and Baldwin [OAMB] improved this
 B728 in 1986 to linear time.²⁵
- B729 • In 1992, Chandran and Mount [ChMo] noted the strong connection between the largest
 B730 inscribed triangle and smallest circumscribed triangle problems, and they succeeded to
 B731 solve both problems simultaneously in linear time.²⁶ At the time, this did not offer any
 B732 improvement over existing algorithms regarding the asymptotic running time. The selling
 B733 point of this paper were fast parallel algorithms for the two problems.
- B734 • In 2017, Keikha, Löffler, Urhausen, and van der Hoog found out that the algorithm of
 B735 Dobkin and Snyder [DS] does not work. Dobkin and Snyder [DS] had promised a proof
 B736 of a crucial lemma in a subsequent full version, but this never appeared. Keikha et al.
 B737 presented a counterexample in the first version of the arXiv preprint [K⁺] in May 2017,
 B738 and they were initially unaware of the previous linear-time solution of Chandran and
 B739 Mount [ChMo]. As a replacement for the incorrect solution, they proposed a divide-and-
 B740 conquer algorithm of running time $O(n \log n)$ for the largest inscribed triangle.
- B741 • The discovery of the mistake in [DS] prompted two linear-time algorithms that were again
 B742 posted as arXiv preprints: By Kallus [Kal], posted in June 2017, and by
 B743 Jin [Jin], whose first version was posted in July 2017. Both papers deal with the largest
 B744 inscribed triangle problem.²⁷ In subsequent versions of [Jin], the smallest circumscribed
 B745 triangle problem is also treated.

References

- B747 [BRS] Peter Braß, Günter Rote, and Konrad J. Swanepoel. Triangles of extremal area or
 B748 perimeter in a finite planar point set. *Discrete and Computational Geometry*, 26:51–
 B749 58, 2001. doi:10.1007/s00454-001-0010-6.
- B750 [ChMo] Sharat Chandran and David M. Mount. A parallel algorithm for enclosed and enclosing
 B751 triangles. *International Journal of Computational Geometry & Applications*, 2(2):191–
 B752 214, 1992. doi:10.1142/S0218195992000123.

B753 ²⁴This algorithm computes the largest triangle anchored to the each inner edge normal. Each triangle is
 B754 computed from scratch in $O(\log^2 n)$ time, as sketched at the beginning of Section 7.

B755 ²⁵This is essentially the algorithm in Section 9.

B756 ²⁶This is the Circular Sweep algorithm in Section 7.

B757 ²⁷The algorithm of Kallus is a rediscovery of the Circular Sweep algorithm of Chandran and Mount [ChMo],
 B758 restricted to the case of the largest inscribed triangle problem. The algorithm of Jin is described in Section 8.2.

B759 [DS] David P. Dobkin and Lawrence Snyder. On a general method for maximizing and mini-
 B760 mizing among certain geometric problems. In *20th Annual Symposium on Foundations*
 B761 *of Computer Science*, pages 9–17. IEEE, 1979. doi:10.1109/SFCS.1979.28.

B762 [Jin] Kai Jin. Maximal area triangles in a convex polygon. Preprint, September 2017.
 B763 arXiv:1707.04071v3.

B764 [Kal] Yoav Kallus. A linear-time algorithm for the maximum-area inscribed triangle in a
 B765 convex polygon. Preprint, June 2017. arXiv:1706.03049.

B766 [K⁺] Vahideh Keikha, Maarten Löffler, Ali Mohades, Jérôme Urhausen, and Ivor van der
 B767 Hoog. Maximum-area triangle in a convex polygon, revisited. Preprint, 2017. arXiv:
 B768 1705.11035v2.

B769 [KILa] Victor Klee and Michael C. Laskowski. Finding the smallest triangles containing a
 B770 given convex polygon. *Journal of Algorithms*, 6(3):359–375, 1985. doi:10.1016/
 B771 0196-6774(85)90005-7.

B772 [OAMB] Joseph O’Rourke, Alok Aggarwal, Sanjeev Maddila, and Michael Baldwin. An optimal
 B773 algorithm for finding minimal enclosing triangles. *Journal of Algorithms*, 7(2):258–269,
 B774 1986. doi:10.1016/0196-6774(86)90007-6.

B775 B Primitive operations

B776 There are two basic operations in the algorithms, besides the calculation and comparison of
 B777 triangle areas:

- B778 1. Constructing the critical pivot point M and comparing it to the edge BC , in order to
 B779 decide in which direction the “current triangle” should be improved.
- B780 2. Finding the next breakpoint when θ is rotated.

B781 Since the first operation is tied to the optimality condition of anchored triangles, this test
 B782 occurs in every algorithm that is based on anchored triangles. As we have seen in Section 8.2, it
 B783 also appears in Jin’s Algorithm, even though Jin’s own derivation [Jin] does not refer to anchored
 B784 triangles at all.

B785 The second operation has to consider the up to three candidates for terminating the current
 B786 interval (see Figure 7) and compare them to see which one is next. This operation also involves
 B787 a critical point M , either as a pivot point or as an obstacle that might be hit by a rotating
 B788 segment. This operation appears only in the original Circular Sweep Algorithm and not in the
 B789 simplified versions that are specialized for the largest inscribed triangle or smallest circumscribed
 B790 triangle.

B791 After introducing the wedge product as a basic operation in Section B.1, we consider the
 B792 two basic operations in Sections B.2 and B.3. In Section B.4, we discuss the degree of the
 B793 algebraic expressions that arise when carrying out the primitive operations on a computer.
 B794 Finally, Section B.5 investigates the degree of the area computation for circumscribed triangles.

B795 B.1 The area of the parallelogram spanned by two vectors

B796 For two vectors or points $\vec{a}_1 = \begin{pmatrix} x_1 \\ y_1 \end{pmatrix}$ and $\vec{a}_2 = \begin{pmatrix} x_2 \\ y_2 \end{pmatrix}$ in the plane, we use the wedge product
 B797 notation for the signed area of the parallelogram spanned by \vec{a}_1 and \vec{a}_2 :

$$B798 \quad \vec{a}_1 \wedge \vec{a}_2 = \begin{vmatrix} x_1 & x_2 \\ y_1 & y_2 \end{vmatrix} = x_1 y_2 - x_2 y_1.$$

B799

B.2 The improvement test for anchored triangles

B800

We first develop the algebra for the Improvement Test (Section B.2.1). In Section B.2.2, we

B801

compare how this test is expressed geometrically in different papers.

B802

B.2.1 Algebraic calculation of the sign of the derivative of $f(h)$

B803

We are given the vertices p_1, p_2, \dots, p_n of the convex n -gon P in counterclockwise order. Indices

B804

are modulo n .

B805

We want to calculate the sign of the one-sided derivative of $f(h)$ at some point h . According to the Improvement Test (conditions (1)–(2)) and the criteria of Lemma 3, this boils down to constructing the points T and M and testing the position of M with respect to BC .

B806

We specify the test by five parameters: three indices i, j, k , the vector \mathbf{u} , and the point A^* .

B807

Their meaning is as follows: B moves on the line through the edge p_i, p_{i+1} and C moves on the line through the edge p_j, p_{j+1} . The current location of the segment BC is specified by one point

B808

p_k through which it goes and by the normal direction \mathbf{u} (pointing to the right of BC). When the test is called, the point p_k is always one of $p_i, p_{i+1}, p_j, p_{j+1}$.

B809

We start by computing the upward vectors $\vec{b} = p_{i+1} - p_i$ and $\vec{c} = p_j - p_{j+1}$. We compute the wedge product

B810

B811

B812

B813

$$\Delta = \vec{c} \wedge \vec{b}.$$

B814

If $\Delta \leq 0$, the forward extensions of \vec{b} and \vec{c} diverge, and the derivative of f is positive. Otherwise, their intersection point is

B815

B816

B817

$$T = \frac{\hat{T}}{\Delta} \tag{5}$$

B818

with

B819

$$\hat{T} = (p_j \wedge p_{j+1}) \cdot \vec{b} + (p_i \wedge p_{i+1}) \cdot \vec{c}.$$

B820

B821

This formula can be worked out by solving the system of linear equations, or it can be checked by computing the products $T \wedge \vec{b}$ and $T \wedge \vec{c}$ and comparing them to what they should be.

B822

To test whether $\frac{T+A^*}{2}$ is above or below BC , we have to check the sign of the scalar product

B823

$(\frac{T+A^*}{2} - p_k) \cdot \mathbf{u}$, which, after multiplying the denominator, becomes

B824

B825

$$S := \left(\hat{T} + (A^* - 2p_k)\Delta \right) \cdot \mathbf{u}. \tag{6}$$

B826

The sign of this expression is the sign of the derivative of $f(h)$.

B827

We can assume that both vectors \vec{b} and \vec{c} have a nonnegative scalar product with \mathbf{u} . Let us first make the additional assumption that at least one vector has a positive scalar product with \mathbf{u} . Then, if $\Delta < 0$, the computed intersection point T lies below A^* , and so does M , but the multiplication by Δ reverses the sign, leading to the correct (positive) sign of S . One can check that S is positive also for $\Delta = 0$. Thus, (6) can be used in all cases, and the sign test of Δ is not necessary. The test covers even the critical point M^{up} when $i = j$ and BC is the \mathbf{u} -extreme edge of P , which does not fall under the initial assumption: In this case, $\vec{c} = -\vec{b}$, $\hat{T} = \binom{0}{0}$, $\Delta = 0$, and $S = 0$, correctly indicating that no improvement is possible by increasing h .

B833

B834

B835

The components of the vector in the large parentheses in (6) have degree 3 in the input variables. When the test is used in the algorithm, the vector \mathbf{u} is typically the perpendicular vector of the next edge incident to A^* or of the vector BC between two vertices of P . The expression (6) has thus degree 4 in the input coordinates.

B836

B837

B838

B839

B.2.2 Geometric constructions of the improvement test

B840

It is interesting to see how this test can be expressed geometrically in different ways. In the algorithms, the test is variously applied to the forward or backward edges incident to B and C . To abstract from these details the tests are illustrated with a smooth convex body P that has unique tangents everywhere. We have also unified the notation, and we don't necessarily use the same wording as in the original sources. Figure 15a shows the test as expressed in this note: Is the critical point $M = (A^* + T)/2$ below or above BC ?

B841

B842

B843

B844

B845

B846

Figure 15b shows the criterion of Klee and Laskowski [KILa, Figure 11], see also [OAMB, Figure 1]: Let h be the height of BC over the tangent \bar{E} at A^* (which is parallel to BC). Now the tangent at C is extended to a point Y that has height $2h$. Then the line YB is formed, and the question is: Does YB intersect the polygon P below B or above B ?

B847

B848

B849

B850

This example is particularly instructive: Our test starts with the given vertices and edges and proceeds by intersecting certain lines or drawing lines through certain points, and in the end, certain distances or locations are compared. In the critical situation, when the outcome of the test changes, there will be some extra incidence. In Figure 15a, the point T would have height $2h$ in the critical situation. Figure 15b performs the construction backwards and makes the comparison at an intermediate stage: It constructs what the tangent at B should be in the critical situation, namely the line YB , and compares it to the actual tangent at B .

B851

B852

B853

B854

B855

B856

B857

This form of the test has the nice feature that it works regardless of whether the upward tangent rays through B and C meet. This is in accordance with the observation from the algebraic calculations in Section B.2.1 that it is not necessary to check whether the rays meet.

B858

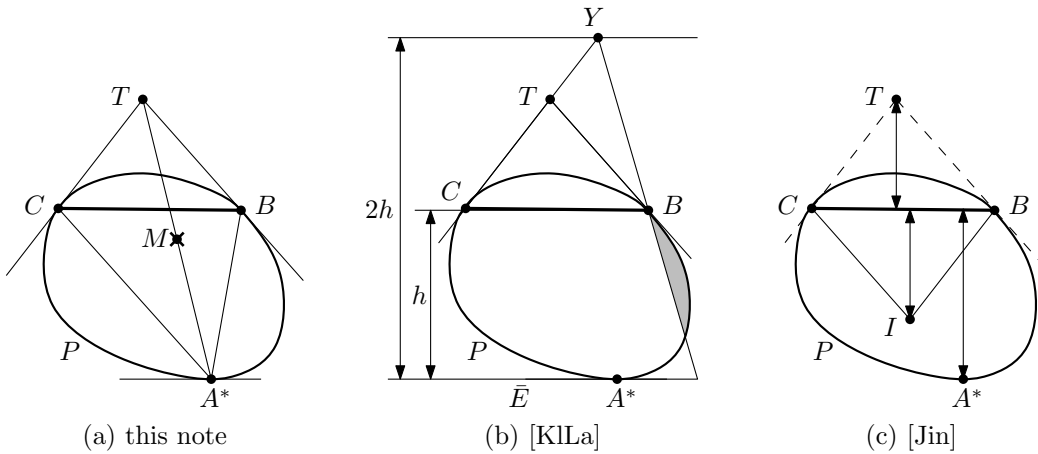
B859

B860

B861

B862

Figure 15c shows the criterion used by Jin [Jin]. It takes the fourth point I of the parallelogram $BTCI$ (without constructing T), and compares the distances of I and A^* from BC . This is obviously equivalent to the test in Figure 15a.



B863

Figure 15: The different geometric ways of expressing the direction of improvement

B864

B.3 Finding the next breakpoint

B.3.1 Algebraic computation of the next breakpoint

B865

B866

B867

B868

B869

B870

For determining the next breakpoint, the three cases with the three candidate directions each are shown in Figure 7. For example, in Case II, we have to compare the directions $next(A) - A$, $M^{down} - C^*$, and $B^{forw} - C^*$, where B^{forw} is the endpoint of $e^{forw}(B)$. Two such vectors are compared by looking at the sign of their wedge product. Two of these directions are directions between two polygon vertices, and hence they come directly from the input data. The challenging case is the vector that involves a critical point. For example, to compare which of the vectors

B871 $M^{\text{down}} - C^*$ and $\text{next}(A) - A$ comes first, we look at the sign of the wedge product $(M^{\text{down}} -$
 B872 $C^*) \wedge (\text{next}(A) - A)$. This is a quadratic expression in the coordinates of the four involved points,
 B873 but since M^{down} involves T^{down} , which is given by the rational expression (5), we multiply by
 B874 Δ . As in (6), the result is a degree-4 polynomial.

B875 Case I is similar. In Case III, it seems that we have to compare two directions that involve M ,
 B876 namely $B^{\text{forw}} - M$ and $M - C^{\text{forw}}$, which would lead to a degree-6 predicate. However, this
 B877 comparison is equivalent to an orientation test for the triangle $B^{\text{forw}}MC^{\text{forw}}$. Thus we can
 B878 compare, for example, $B^{\text{forw}} - C^{\text{forw}}$ against $B^{\text{forw}} - M$ to get a degree-4 test with an equivalent
 B879 outcome.

B880 Summarizing, we have shown that the selection of the next event can be done by evaluating
 B881 the signs of polynomials of degree at most 4 in the input coordinates.

B882 B.3.2 Computation and construction of the next breakpoint in the literature

B883 As in Section B.2.2, we want to compare how these tests are expressed in the literature. Two
 B884 papers have suggested the conceptual sweep through all angles θ : Chandran and Mount [ChMo],
 B885 and Kallus [Kal].

B886 Kallus [Kal, Theorem 6] describes the necessary tests purely in algebraic terms, by setting
 B887 derivatives to 0, without distilling the geometric content. [Kal, Listing 3] spells out the formulas
 B888 for all primitives. Some of these expressions are rational expressions with numerator and denom-
 B889 inator of degree 4, and they are compared against other rational expressions with numerator
 B890 and denominator of degree 2. The comparison amounts to computing the sign of a degree-6
 B891 polynomial. So it appears that these expressions are not optimized.

B892 Chandran and Mount’s algorithm [ChMo], by contrast, is described in geometric terms, and
 B893 we can compare their description to ours. Indeed, when both B^* and C^* move (Case III), they
 B894 construct the point M around which B^*C^* rotates. This is [ChMo, Figure 5], covering the case
 B895 where the outer triangle has “two flush legs”. (The pivot is the point x in that figure, and it
 B896 is constructed by considering the local optimality condition of the corresponding circumscribed
 B897 triangle.)

B898 The case of “one flush leg” covers Case I and II of Figure 7, where one point B^* or C^*
 B899 remains at a vertex. The interesting event is that B^*C^* hits a critical point M . Figure 16
 B900 shows the test of [ChMo, Figure 6] for Case II, converted to our notation and our conventions.
 B901 The construction extends the line from the intersection point T^{down} of the tangents towards the
 B902 point C^* , going twice the distance $T^{\text{down}}C^*$, and arriving at the point y . The direction where
 B903 the critical event happens is determined by the line A^*y . Again, this criterion is found from the
 B904 local optimality condition of the circumscribed triangle. Clearly, as the triangles $T^{\text{down}}C^*M^{\text{down}}$
 B905 and $T^{\text{down}}yA^*$ are similar, this is the same direction as C^*M^{down} .

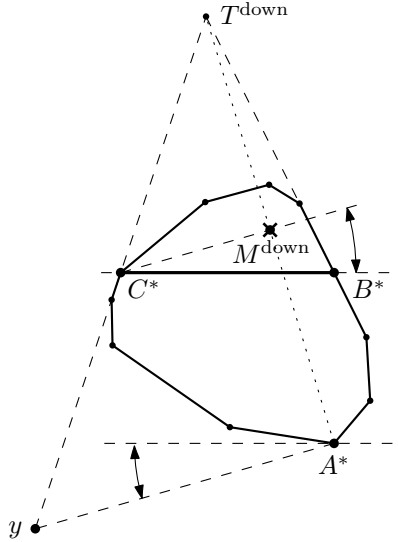
B906 B.4 The degree of the predicates

B907 As we have seen, the Improvement Test boils down to a sign test for a degree-4 polynomial. The
 B908 degree is important when predicates are evaluated exactly, because it determines the blow-up of
 B909 the involved numbers. The problem *statement* of the largest inscribed triangle, however, refers
 B910 only the computation and comparison of triangle areas, which is an easy degree-2 operation.

B911 All known linear-time algorithms require the Improvement Test in one form or another.
 B912 There is an algorithm to compute the largest inscribed triangle in $O(n \log n)$ time, which only
 B913 compares triangle areas $[K^+]$. Is there a linear-time algorithm that avoids degree-4 predicates?

B914 B.5 The area of the circumscribed triangle

B915 As for circumscribed triangles, Klee and Laskowski [KLLa] advertise their algorithm for finding
 B916 all local minima of circumscribed triangles with the following words: “It does not compute any



B917 Figure 16: Two different geometric ways of finding the next event in Case II, when B^*C^* rotates
 B918 around C^*

B919 areas, but relies on a geometric characterization of the local minima and on simple computational
 B920 steps such as finding intersections of lines.” Actually, for circumscribed triangles, this is a
 B921 justified remark, because the area of a triangle that is given by edges is not so nice to compute
 B922 as when the vertices are given, and this is reflected in the algebraic degree. Consider a triangle
 B923 where each side is specified by two points (x_i, y_i) and (u_i, v_i) through which it goes, for $i =$
 B924 $1, 2, 3$. Such a triangle, touching three edges of the input polygon P , can arise as a smallest
 B925 circumscribed triangle. Its area is the following rational expression whose numerator has degree 8
 B926 and whose denominator has degree 6:

$$\pm \frac{\begin{vmatrix} x_1v_1 - y_1u_1 & x_1 - u_1 & y_1 - v_1 \\ x_2v_2 - y_2u_2 & x_2 - u_2 & y_2 - v_2 \\ x_3v_3 - y_3u_3 & x_3 - u_3 & y_3 - v_3 \end{vmatrix}^2}{2 \cdot \begin{vmatrix} x_1 - u_1 & y_1 - v_1 \\ x_2 - u_2 & y_2 - v_2 \end{vmatrix} \cdot \begin{vmatrix} x_2 - u_2 & y_2 - v_2 \\ x_3 - u_3 & y_3 - v_3 \end{vmatrix} \cdot \begin{vmatrix} x_3 - u_3 & y_3 - v_3 \\ x_1 - u_1 & y_1 - v_1 \end{vmatrix}}$$

B927 This formula was calculated with the help of a computer algebra system. To compare two such
 B928 areas exactly requires the evaluation of the sign of a degree-14 polynomial in the input variables.

B929 There is another case, when the smallest circumscribed triangle has just two “flush sides”.
 B930 The definition of such a triangle involves only 5 input points, and it can be worked out by hand.
 B931 If the third side goes through the point (x_3, y_3) and the other two sides are specified as before,
 B932 numerator of the area has degree 4 and the denominator has degree 2:

$$\pm 2 \cdot \frac{\begin{vmatrix} x_2 - x_3 & y_2 - y_3 \\ x_2 - u_2 & y_2 - v_2 \end{vmatrix} \cdot \begin{vmatrix} x_1 - x_3 & y_1 - y_3 \\ x_1 - u_1 & y_1 - v_1 \end{vmatrix}}{\begin{vmatrix} x_1 - u_1 & y_1 - v_1 \\ x_2 - u_2 & y_2 - v_2 \end{vmatrix}}$$

B934 C Constructing the largest anchored inscribed triangle from the smallest anchored circumscribed triangle

Here is the converse statement to Lemma 4.i.

B935 **Lemma 14.** Let $\hat{A}\hat{B}\hat{C}$ be a smallest circumscribed triangle anchored at $-\mathbf{u}$, of height \hat{h} . Then
 B936 the largest inscribed triangle $A^*B^*C^*$ anchored at \mathbf{u} has vertices $B^* = (\hat{A} + \hat{C})/2$ and $C^* =$
 B937 $(\hat{A} + \hat{B})/2$, and the vertex A^* lies on the side $\hat{B}\hat{C}$ (see Figure 5b). Hence it has height $h = \hat{h}/2$,
 B938 and the length of its baseline is $B^*C^* = \hat{B}\hat{C}/2$, and its area is $1/4$ of the area of $\hat{A}\hat{B}\hat{C}$.²⁸

B939 The proof hinges on the well-known optimality condition for circumscribed triangles:

B940 **Lemma 15.** Let $\hat{O}\hat{X}\hat{Y}$ be a smallest triangle containing a convex polygon P under the constraint
 B941 that \hat{O} is fixed and \hat{X} and \hat{Y} lie on two given rays emanating from \hat{O} . Then the midpoint
 B942 $(\hat{X} + \hat{Y})/2$ touches P .²⁹

B943 *Proof.* Clearly, the side $\hat{X}\hat{Y}$ must touch P . If it does not touch P at the midpoint $(\hat{X} + \hat{Y})/2$,
 B944 then the area can be decreased by tilting the side $\hat{X}\hat{Y}$ around the vertex where it touches P .
 B945 This has been implicitly shown in the proof of Lemma 6, see Figure 9b with TC^*B^* in the role
 B946 of $\hat{O}\hat{X}\hat{Y}$. If the side $\hat{X}\hat{Y}$ touches an edge of P , we tilt it around the endpoint closer to the
 B947 midpoint. \square

B948 *Proof of Lemma 14.* It is obvious that A^* lies on the side $\hat{B}\hat{C}$. By Lemma 15, applied to
 B949 $\hat{O}\hat{X}\hat{Y} = \hat{B}\hat{C}\hat{A}$ and $\hat{O}\hat{X}\hat{Y} = \hat{C}\hat{A}\hat{B}$, the midpoints $B^* = (\hat{A} + \hat{C})/2$ and $C^* = (\hat{A} + \hat{B})/2$ of the
 B950 two “legs” $\hat{A}\hat{C}$ and $\hat{A}\hat{B}$ lie in P .

B951 Optimality of $A^*B^*C^*$ within P follows easily by Lemma 2: An anchored triangle larger
 B952 than $A^*B^*C^*$ cannot even be found in the circumscribed triangle $\hat{A}\hat{B}\hat{C} \supseteq P$. \square

B953 D An alternative proof that B^* and C^* move monotonically

B954 We have proved the monotone movement of the points $B^*(\theta)$ and $C^*(\theta)$ as a consequence of
 B955 the analysis of the possible local movements at each direction in Theorem 5. We will give an
 B956 independent self-contained proof.³⁰

B957 **Lemma 16.** As θ increases, each of the points $B^*(\theta)$ and $C^*(\theta)$ moves only in the forward
 B958 direction (or stays where it is).

B959 *Proof.* It is enough to prove monotonicity for some range of directions θ where A^* is constant.

B960 It is impossible that none of B^* and C^* moves forward, because then the segment B^*C^* would
 B961 stay the same or turn clockwise while its supposed normal direction $\mathbf{u}(\theta)$ turns counterclockwise.

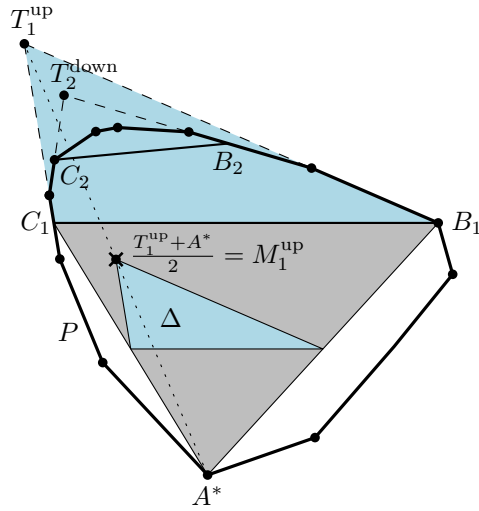
B962 Thus, we are left to exclude the case that one of the points B^* and C^* moves backward
 B963 and the other moves forward. If this happens, then there are two values $\theta_1 \neq \theta_2$ such that the
 B964 four points $B_1 = B^*(\theta_1), C_1 = C^*(\theta_1), B_2 = B^*(\theta_2), C_2 = C^*(\theta_2)$ are distinct and occur in the
 B965 clockwise order $B_1B_2C_2C_1$ on the boundary, see Figure 17.

B966 Let us look at the edges $e^{\text{forw}}(B_1)$ and $e^{\text{back}}(C_1)$. By the optimality criterion, their upward
 B967 extensions intersect in some point T_1^{up} , and the critical pivot point $M_1^{\text{up}} = (T_1^{\text{up}} + A^*)/2$ lies on
 B968 or below the line B_1C_1 . The edges $e^{\text{back}}(B_2)$ and $e^{\text{forw}}(C_2)$ lie between $e^{\text{forw}}(B_1)$ and $e^{\text{back}}(C_1)$
 B969 in the cyclic order, with equality permitted. Hence, their intersection point T_2^{down} lies in the
 B970 triangle $B_1C_1T_1^{\text{up}}$. This restricts the critical pivot point $M_2^{\text{down}} = (T_2^{\text{down}} + A^*)/2$ of $A^*B_2C_2$
 B971 to a smaller triangle Δ that is dilated from the center A^* with a factor $\frac{1}{2}$. The triangle Δ has
 B972 its top vertex at M_1^{up} , and its lower edge is parallel to B_1C_1 . It follows that M_2^{down} lies on or
 B973 below B_1C_1 , and therefore strictly below B_2C_2 , and hence B_2C_2 is not optimal. \square

B974 ²⁸Chandran and Mount [ChMo, Lemma 2.4] proved that there is always an “inner triangle” $A^*B^*C^*$ that
 B975 satisfies all the geometric relations stated in Lemma 14, without noting (or caring to state) that $A^*B^*C^*$ is the
 B976 largest anchored inscribed triangle. In a separate lemma [ChMo, Lemma 2.5(ii)], they proved only that the overall
 B977 largest inscribed triangle arises as the inner triangle of some (special) smallest anchored circumscribed triangle.
 B978 In this case, the inner triangle is even a homothetic copy of the circumscribed triangle, scaled with the factor $-\frac{1}{2}$.

B979 ²⁹This condition is also sufficient for optimality in the setting of this lemma, see [KILa, Lemma 1.2].

B980 ³⁰See also the “interspersing property” in [OAMB, Lemma 2]. The “interleaving property” in [K⁺, Lemma 5]
 B981 is similar, but it holds for a different class of triangles, the so-called “3-stable” triangles.



B982 Figure 17: Proof of Lemma 16. In this example, $\theta_1 < \theta_2$. The proof works equally when the
 B983 opposite relation holds.

B984 As a consequence of this lemma, one can conclude that the motion of $B^*(\theta)$ and $C^*(\theta)$ is
 B985 continuous, because a discontinuity would be inconsistent with monotonicity, given that the
 B986 direction changes continuously. The case when B^*C^* is the \mathbf{u} -extreme edge of P must be
 B987 considered separately for this argument.

B988 Continuity can also be established directly from basic properties of the underlying optimiza-
 B989 tion problem [Kal, Lemma 3.2].

B990 We have used continuity as part of Theorem 5 only to establish monotonicity, but otherwise,
 B991 the algorithm does not depend on continuity. However, if continuity can be assumed, this would
 B992 simplify some arguments in the proof of Theorem 5.